

Quantifying errors of electron-proton/muon correlation functionals through the Kohn-Sham inversion of a two-component model system

Nahid Sadat Riyahi ¹, Mohammad Goli ^{2,*} and Shant Shahbazian ^{3,4,†}

¹*Department of Physical and Computational Chemistry, Shahid Beheshti University, Evin, Tehran 19839-69411, Iran*

²*School of Nano Science, Institute for Research in Fundamental Sciences (IPM), Tehran 19395-5531, Iran*

³*Department of Physics, Shahid Beheshti University, Evin, Tehran 19839-69411, Iran*

⁴*Department of Chemistry, Sharif University of Technology, Tehran 11155-9516, Iran*



(Received 5 October 2023; revised 7 November 2023; accepted 30 November 2023; published 22 December 2023)

The multicomponent density functional theory is faced with the challenge of capturing various types of inter- and intraparticle exchange-correlation effects beyond those introduced by the conventional electronic exchange-correlation functionals. Herein, we focus on evaluating the electron-proton/muon correlation functionals appearing in molecular/condensed-phase systems where a proton/muon is treated as a quantum particle on equal footing with electrons, beyond the Born-Oppenheimer paradigm. Five recently developed local correlation functionals, i.e., the epc series and euc-1, are selected and their performances are analyzed by employing a two-particle model that includes an electron and a positively charged particle (PCP) with a variable mass, interacting through Coulombic forces, within a double harmonic trap. Using the Kohn-Sham (KS) inversion procedure, the exact two-component KS characterization of the model is deduced and its properties are compared to those derived from the considered functionals. The analysis demonstrates that these local functionals achieve their original parameterization objectives to reproduce the one-PCP densities and the electron-PCP correlation energies, but all fall short of reproducing the underlying PCP correlation potentials correctly. Moreover, a comprehensive error analysis reveals that the density-driven errors have a non-negligible contribution to the success of the considered functionals. Overall, the study shows the strengths as well as shortcomings of the considered functionals hopefully paving the way for designing more robust functionals in the future.

DOI: [10.1103/PhysRevB.108.245155](https://doi.org/10.1103/PhysRevB.108.245155)

I. INTRODUCTION

The last two decades have witnessed a new age in *ab initio* computational study of the multicomponent Coulombic quantum systems which has been recently called the multicomponent quantum chemistry (MCQC) [1]. The MCQC aims to extend the applicability domain of *ab initio* QC to molecular systems and phenomena where not only electrons but also other particles are treated as quantum particles. Apart from the usual light nuclei like proton and its heavier isotopes, this includes elementary particles that are attached to molecular systems like positron or the positively charged muon (hereafter called muon for brevity) [2–15]. While there is a “prehistory” for this extension [16–20], in one sense the renaissance of the MCQC started from the pioneering work of Tachikawa, Nakai, Shigeta, and coworkers in 1998 [21–24]. These studies laid the stepping stone to attribute and optimize spin-spatial orbitals simultaneously to electrons as well as nuclei and/or other elementary particles in molecular systems. Since then various research groups have tried to bring the traditional hierarchical structure of the electronic *ab initio* methodologies, i.e., first Hartree-Fock (HF) and then step by step more sophisticated post-HF methods, to the realm

of the MCQC [25–31]. At first glance this may seem to be a computationally cumbersome but theoretically straightforward research program without any need for innovative theoretical elements. However, this is deceptive since new types of correlations emerge in such systems apart from the well-known electron-electron correlation [32,33].

Let us imagine a two-component system composed of N electrons and a single positively charged particle (PCP), all within an external field. The MCHF wave function, as the starting point for *ab initio* calculations, is a product of the electronic $N \times N$ Slater determinant and the spin-orbital attributed to the PCP, which is an uncorrelated description of electrons and the PCP. Neglecting all types of correlations among the involved particles leads to a significant difference in the observable results computed at the MCHF level compared to the exact solution of the MC-Schrödinger equation [34,35]. Inevitably, in subsequent steps in any conceived hierarchical structure of the MCQM, one must deal with both electron-electron and electron-PCP correlations and try to incorporate them efficiently into the wave function. Nevertheless, the electron-PCP correlation is not only quantitatively but also qualitatively different from the electron-electron correlation because an electron and a PCP form a distinguishable and *attractively* interacting pair of particles with no operative exchange phenomenon, unlike electrons. In fact, two decades of experience reveal that the orbital-based *ab initio* correlated methods, which are capable of recovering electron-electron

*m_goli@ipm.ir

†sh_shahbazian@sbu.ac.ir, sh-shahbazian@sharif.edu

correlation, are not suitable to recover the electron-PCP correlation efficiently and new methodological developments are necessary [36–66]. This is also the case for the extension of density functional theory (DFT) to the MC systems as one of the most computationally cost-effective methodologies to deal with the many-body problem [67]. While the theoretical foundations of the MCDFT were laid decades ago [68–77], and refined since then [78–89], properly designed electron-PCP correlation functionals have appeared only recently [90–108]. Although it is not discussed in the present study, let us just briefly stress that another type of correlation, namely the PCP-PCP correlation, may also emerge if, for example, one considers quantum systems composed of N electrons and M PCPs when $M > 1$. Probably, the most interesting example is hydrogen under extreme pressures and its infamous metallic phase [109–112], which is basically a strongly interacting system of electrons and protons (or deuteriums) [113–124]. Accordingly, in an *ab initio* study of an MC many-body quantum system, composed of quantum particles with different charges and masses, the diversity of various conceived correlations is enormous. Currently, in contrast to all attempts [125–136], there is no single unified scheme to treat all these correlations efficiently and much remains to be done in this area.

In the meantime, the most computationally tractable *ab initio* methodology to deal with medium to large MC molecular systems is the MCDFT and the solution of the MC Kohn-Sham (MCKS) equations. The recent success in introducing relatively accurate local and semilocal electron-positron [90,100,102], electron-proton [104,105,107], and electron-muon [108], correlation functionals are indeed promising. However, designing novel correlation functionals is by no means a straightforward task since the goal of building a simplified but reliable many-body model to start considering the electron-PCP correlation, similar to the homogeneous electron gas model used in the electronic DFT (eDFT) [137,138], is not achieved yet. The only exception is the “delocalized” states of positrons in solids [3], for which the many-body homogeneous electron-positron gas model was developed long ago [139–144]. This model has been employed to deduce local density approximations for the electron-positron correlation functional [145–147]. While the model has been extended to the case of a PCP with an arbitrary mass [148–154], the “localized” nature of the heavy PCPs, e.g., proton and muon, in many MC systems cast some doubt on the model’s validity in such cases. As an alternative, the recently designed electron-proton correlation functionals have been largely based on extending the Colle-Salvetti approximation for the electron-electron correlation energy [155,156], to the electron-proton correlation energy [104,105,107]. Although some theoretical clarifications yet needed to be done in this procedure, the computational success of the series of designed functionals, called epc-17 [104], epc-18 [105], and epc-19 [107], encourages this line of reasoning [1,157–159]. The epc-1 functional [108], which is recently proposed to account for the electron-muon correlation effects, resembles the epc series mathematically, but simply designed based on a semiempirical approach from the outset (see Appendix C). Accordingly, it is desirable to check the intrinsic accuracy of these functional and try to uncover the reasons behind their success. By the way,

this is not a straightforward task, since in an *ab initio* MCDFT calculation the outcomes, e.g., total energy or geometrical parameters, depend both on the qualities of the electronic exchange-correlation and the electron-PCP correlation functionals. A handful of studies on the possible inter-dependence of these two types of correlations have come to opposing views, and further studies are needed for more clarification [99,101,105]. Nevertheless, all the mentioned electron-PCP functionals have been parameterized in *ab initio* procedures on real molecules employing the same electronic exchange-correlation functionals that are used in the “single-component” eDFT without any re-parameterization. A reasonable doubt emerges as to what extent the electron-PCP correlation functionals “absorb” the errors inherent in the original design of the electronic exchange-correlation functionals. In fact, the error compensation of two seemingly independent functionals that are used in conjunction with *ab initio* calculations is well-documented and has been utilized in the joint parameterization of the electronic exchange and correlation functionals [160].

Currently, the “gold standard” for the quality of an electron-PCP correlation functional is its ability to overcome the *overlocalization* of the uncorrelated one-PCP density (*vide infra*). These overlocalized uncorrelated densities are derived from MCKS (and MCHF) wave functions in the absence of the electron-PCP correlation functional [104,105,107,108]. However, these studies demonstrate that the “cure” of the overlocalization does not in itself guarantee the success of an electron-PCP correlation functional in reproducing the correct energetics. Thus it is desirable to find new ways of gauging the “inherent” accuracy of the currently used electron-PCP correlation functionals. To reach this goal, it is preferable to apply the MCKS equations with the desired electron-PCP correlation functional to a model system that lacks the electron-electron and PCP-PCP correlations. Such a system is inevitably composed of just one electron and a PCP, all placed within an external field, to eliminate the unbound center of mass motion preventing concomitant complications [161].

The following section presents the basic theory of this model system and shows that the overlocalization problem persists in this system regardless of whether the PCP is a proton or a muon. Thus this simple model is a proper testing ground to evaluate the quality of the electron-PCP correlation functionals. Also, various energetic comparisons are done comparing the results of the exact MCKS with those derived from various local correlation functionals including, the electron-PCP correlation energy and the KS potentials of the electron and the PCP. Overall, the present study tries to evaluate the inherent qualities of the local electron-proton and electron-muon correlation functionals currently in use.

II. THE MODEL TWO-PARTICLE SYSTEM

A. The theoretical basics

The idea of using simple models to evaluate the correlation energies in many-body systems, i.e., the difference between the exact and the mean-field energies, is not new and its usefulness has been demonstrated many times previously [162–165]. In the case of electron-electron correlation, probably the best-known and the most studied model is the

two-electron harmonium atom, sometimes also called the Hooke's atom, which is composed of two electrons interacting within a harmonic trap [166]. The model was first proposed by Kestner and Sinanoglu in 1962 [167], as a simplified version of the real helium atom, and since then it has been studied by various researchers [168–200]. In contrast to the helium atom, the partial electronic Schrödinger differential equation of the harmonium atom is separable into two ordinary differential equations [167]. One of them is equivalent to the Schrödinger equation of the harmonic oscillator problem, and is analytically solvable, while the other belongs to the class of quasireactly solvable models [167,168,172,175,201]. Since the exact analytical and/or numerical solutions of these equations are available, the model is an ideal “laboratory” to study the electron correlation effects. One of the most interesting applications of this laboratory is the evaluation of the reliability of various proposed approximate electronic exchange-correlation functionals used in the eDFT. The exact noninteracting KS system of the harmonium atom and its components, e.g., the KS correlation energy and the exchange-correlation potential, are derivable from an inversion process. Hence, the exact components are comparable with their approximate counterparts, derived from the approximate exchange-correlation functionals [202]. The pioneering studies of Laufer and Krieger in 1986 [203], as well as other researchers [204–208], set the stage for subsequent studies on various aspects of the eDFT of the harmonium atom [209–241]. Accordingly, it is desirable to have a similar model to study the electron-PCP correlation-related effects and to evaluate the utility of the recently designed electron-PCP correlation functionals.

To construct the proper model, one of the two electrons in the harmonium model is replaced with a particle having a unit of the positive charge and an arbitrary mass (equal to or larger than the electron's mass). Our previous studies indeed revealed that in real molecules, on average, a single electron surrounds a proton/muon thus the model hopefully must simulate hydrogen (H)/muonium (Mu) atom bonded within a molecule [242–245]. The corresponding Hamiltonian of the model, hereafter called the H/Mu atom in the double harmonic traps, and abbreviated as H/Mu-DHT, is as follows:

$$\begin{aligned} \hat{H} &= \hat{T}_e + \hat{T}_{\text{PCP}} + \hat{V}_{e\text{-PCP}} + v_e^{\text{ext}}(\vec{r}_e) + v_{\text{PCP}}^{\text{ext}}(\vec{r}_{\text{PCP}}) \\ &= -\frac{1}{2}\nabla_e^2 - \frac{1}{2m_{\text{PCP}}}\nabla_{\text{PCP}}^2 - \frac{1}{|\vec{r}_e - \vec{r}_{\text{PCP}}|} \\ &\quad + \frac{1}{2}k_e r_e^2 + \frac{1}{2}k_{\text{PCP}} r_{\text{PCP}}^2. \end{aligned} \quad (1)$$

Note that both in this equation and throughout the rest of the text, all equations and numerical data are given in the atomic units unless stated otherwise. The parameters of the model are the mass of the PCP, m_{PCP} , and the force constants of the two traps, one for the electron, k_e , and the other for the PCP, k_{PCP} , sharing a single center in space. Each trap acts as the external potential for the electron, v_e^{ext} , or the PCP, $v_{\text{PCP}}^{\text{ext}}$. A special case of this model, $k_e = 0$, has been considered recently [246], but since we are interested in a separable Hamiltonian (*vide infra*), we further assume that the frequency of oscillations is equal for the two traps: $k_i = m_i \omega^2$. Let us stress at this stage of development that the model can be used to simulate various

physical systems that some are beyond the intent of the present study including the trapped atoms [247–250], and the electron-hole pair [251–256]. The Hamiltonian is transformed by employing the center of mass, $\vec{R} = (\vec{r}_e + m_{\text{PCP}}\vec{r}_{\text{PCP}})/M$, and the relative, $\vec{r} = \vec{r}_e - \vec{r}_{\text{PCP}}$, variables into two independent Hamiltonians without any coupling term:

$$\begin{aligned} \hat{H} &= \hat{H}_R + \hat{H}_r, \\ \hat{H}_R &= -\frac{1}{2M}\nabla_R^2 + \frac{1}{2}M\omega^2 R^2, \\ \hat{H}_r &= -\frac{1}{2\mu}\nabla_r^2 + \frac{1}{2}\mu\omega^2 r^2 - \frac{1}{r}. \end{aligned} \quad (2)$$

The center of mass Hamiltonian, \hat{H}_R , describes a pseudoparticle with the total mass $M = 1 + m_{\text{PCP}}$, in a harmonic trap which is a textbook example of an analytically solvable model [257]. The relative motion Hamiltonian, \hat{H}_r , describes a pseudoparticle with the reduced mass $\mu = m_{\text{PCP}}/(1 + m_{\text{PCP}})$, experiencing a harmonic potential and a Coulombic attraction. The mathematical procedures used to derive the analytical solutions of the relative motion Hamiltonian of the harmonium atom do not provide us with the analytical solution for the ground state of \hat{H}_r [175,187,195,201]. Accordingly, for different sets of the model's parameters, we derived the ground state wave functions of the relative motion from high-precision numerical solutions through the finite element method.

To test the physical relevance of the model, the mass and the frequency of oscillation of the model must be fixed to values that make comparison to real physical systems feasible. Since in this study, we are interested in the correlations between localized PCPs and electrons, the mass of the PCP was fixed at the masses of proton, $m_{\text{proton}} \approx 1836$, and muon, $m_{\text{muon}} \approx 207$. Fixing the frequency of oscillation and concomitant force constants is a more delicate issue, since, based on the separability condition of the Hamiltonian, the frequency of oscillation must be equal for the electron and the proton/muon. In fact, the force constants may be viewed as a simple representation of how the other nuclei and electrons collectively affect the target electron and the proton/muon in a real molecule. It seems reasonable to assume that the target electron is mainly influenced by the nearby proton/muon and is least affected by other nuclei/electrons and this justifies the assumption $k_e = 0$ [246]. However, in principle, any other value for the force constant that makes it small relative to the Coulomb term in the vicinity of the center of the trap is also physically a reasonable choice. We fixed the frequency of oscillation by taking into account the typical known values of the zero-point vibrational energies of proton/muon in real molecules, $\omega_{\text{proton}} = 0.01$ and $\omega_{\text{muon}} = 0.02$ [258,259]. With this strategy, since the force constants are scaled with the particle's mass, $k_i = m_i \omega^2$, the relative smallness of k_e is guaranteed. Nevertheless, the main results gained in this study are not sensitive to the numerical choice of ω and remain valid in a broad range of oscillation frequencies.

B. The overlocalization of the uncorrelated one-proton/muon densities

In the first step, the exact and the mean-field derived one-proton/muon densities were studied to see whether the

previously mentioned overlocalization is taking place also in the model. This is a crucial characteristic without which the model would not be proper for the quality evaluation of the electron-PCP correlation functionals. The one-particle densities in the original variables are easily deducible from the exact ground state wave function of the model: $\rho_e(\vec{r}_e) = \int d\vec{r}_{p/\mu} |\Psi_{\text{exact}}(\vec{r}_e, \vec{r}_{p/\mu})|^2$, $\rho_{p/\mu}(\vec{r}_{p/\mu}) = \int d\vec{r}_e |\Psi_{\text{exact}}(\vec{r}_e, \vec{r}_{p/\mu})|^2$. Note that since Eq. (2) is solved in practice, the ground state wave function is derived according to the secondary variables, $\Psi(\vec{r}, \vec{R})$. Therefore, before doing the integration, a “back transformation” must be done to the original variables where its mathematical details have been disclosed previously by Laufer and Krieger and are not reiterated herein [203]. The derived one-particle densities are the “reference” densities of the model for all subsequent comparisons.

To check the presence of the overlocalization in $\rho_{p/\mu}$ of the model, as discussed previously, we need to have also an uncorrelated description of the electron and the proton/muon. Accordingly, we tried to find the best variational Hartree-product solution for the ground state of the model, $\Psi_{\text{uncorrelated}}(\vec{r}_e, \vec{r}_{p/\mu}) = \phi_e(\vec{r}_e)\phi_{p/\mu}(\vec{r}_{p/\mu})$, which is formally equivalent to the MCHF wave function for a system composed of an electron and a proton/muon. This was done by expanding ϕ_e and $\phi_{p/\mu}$ in a series of seven s-, p-, and d-type Gaussian functions denoted as [7s7p7d/7s7p7d] basis set; details of the basis set are given in Appendix A. It was found during the numerical tests that the MCHF/[7s7p7d/7s7p7d] level yields numerical results near the infinite basis limit for the practical applications intended in this study. From the derived uncorrelated wave function, the uncorrelated one-particle densities are easily deducible: $\rho_e = |\phi_e|^2$ and $\rho_{p/\mu} = |\phi_{p/\mu}|^2$. For comparison purposes, the same one-particle densities were also computed for hydrogen/muonium cyanide, XCN ($X=H, \text{Mu}$), where the latter is the simplest muonic molecule considered in our previous MCDFT study [108]. The details of the used computational levels to deduce the reference/exact and uncorrelated one-particle densities may be found in our previous paper [108], and a brief survey is also given in Appendix B.

Figures 1 and 2 depict 1D slices of the one-particle densities computed from the exact and uncorrelated wave functions for the model and the XCN molecules. In the case of the model, since the one-particle densities are isotropic, the axis used to depict the figures is arbitrary and goes through the joint center of the traps, whereas for XCN species, they are anisotropic and the axis passes through the maximum of $\rho_{p/\mu}$ and the clamped carbon and nitrogen nuclei is used for depiction [108]. A quick glance at Fig. 1 reveals unequivocally the expected overlocalization of the uncorrelated $\rho_{p/\mu}$ in comparison to the reference densities in both real and model systems, whereas no such extreme overlocalization is observable in the case of ρ_e in Fig. 2.

We conclude that the model, in contrast to its seemingly profound simplicity, reveals the same pathological behavior of the uncorrelated $\rho_{p/\mu}$ observable in the case of the real systems. In this regard, it can be used as a laboratory to study this “pathological behavior” in detail and to verify how a properly designed correlated wave function, or an electron-proton/muon correlation functional, may remedy the overlocalization.

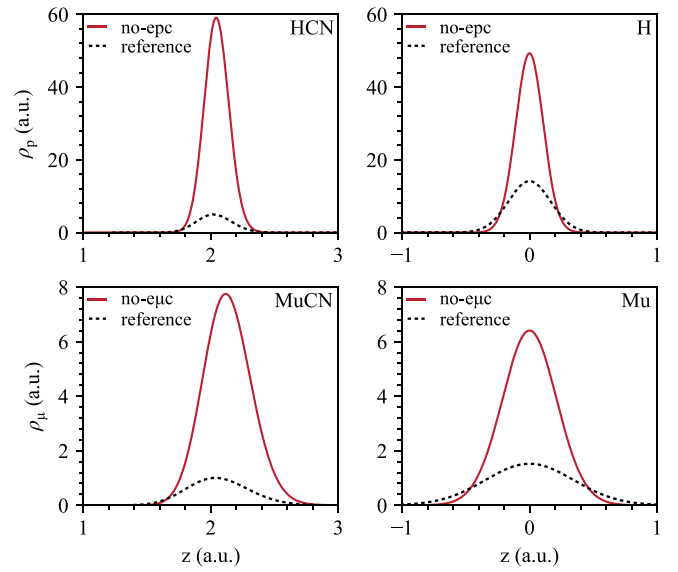


FIG. 1. The left-hand panels depict $\rho_{p/\mu}$ for HCN and MuCN, while the right-hand panels depict the same densities for H/Mu-DHT. The reference $\rho_{p/\mu}$ of HCN and MuCN, depicted as dashed curves, were derived in a previous study from the double-adiabatic approximation [108]. The reference $\rho_{p/\mu}$ for the model, depicted as dashed curves, is obtained from the computed exact wave function. The uncorrelated one-particle densities of the model, the solid red curves, are obtained at the MCHF/[7s7p7d/7s7p7d] level while for HCN and MuCN they are derived at the B3LYP/pc-2//no-epc/14s14p14d and B3LYP/pc-2//no-epc/14s14p14d levels (for more details see Appendix B). In the case of the model, all the one-particle densities are isotropic and the center of the coordinate system is placed at the joint center of the traps. For the real molecules, the one-particle densities are anisotropic and the axis used to depict the densities goes through the maximum of $\rho_{p/\mu}$ and the clamped carbon while the latter is located at the center of the coordinate system.

C. The two-component KS inversion

As discussed in the introduction, the fundamental theorems of the MCDFT as well as the MCKS equations have been derived for the general MC systems long ago (for a compressed review see Sec. 9.6 in Ref. [137]). By the way, in this subsection, we briefly review the specific KS system of the model and also the inversion process upon which the exact electron-proton/muon correlational potential is derived. Numerical comparisons with approximate correlation functionals are considered in the next section.

The MC Hohenberg-Kohn theorems and the generalized Levy’s constraint search imply the following for finding the ground state energy of the model based on Eq. (1):

$$\begin{aligned}
 E_{\text{ground}} &= \min_{\rho_e, \rho_{p/\mu}} E[\rho_e, \rho_{p/\mu}], \\
 E[\rho_e, \rho_{p/\mu}] &= F[\rho_e, \rho_{p/\mu}] + \int d\vec{r}_e v_e^{\text{ext}}(\vec{r}_e) \rho_e(\vec{r}_e) \\
 &\quad + \int d\vec{r}_{p/\mu} v_{p/\mu}^{\text{ext}}(\vec{r}_{p/\mu}) \rho_{p/\mu}(\vec{r}_{p/\mu}), \\
 F[\rho_e, \rho_{p/\mu}] &= \min_{\Psi_{e,p/\mu} \rightarrow \rho_e, \rho_{p/\mu}} \langle \Psi_{e,p/\mu} | \hat{T}_e + \hat{T}_{p/\mu} + \hat{V}_{e-(p/\mu)} | \Psi_{e,p/\mu} \rangle \\
 &= T_e[\rho_e, \rho_{p/\mu}] + T_{p/\mu}[\rho_e, \rho_{p/\mu}] + V_{e-(p/\mu)}[\rho_e, \rho_{p/\mu}].
 \end{aligned} \tag{3}$$

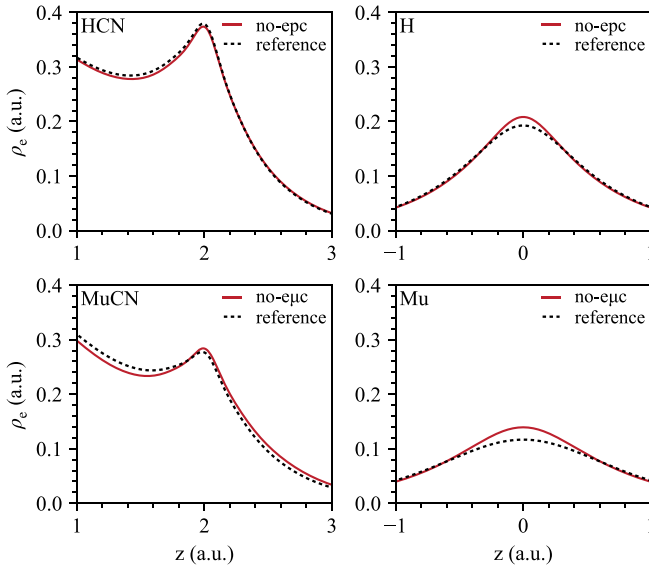


FIG. 2. The left-hand panels depict ρ_e for HCN and MuCN, while the right-hand panels depict the same densities for H/Mu-DHT. The reference ρ_e of HCN and MuCN, depicted as dashed curves, are computed at the B3LYP/pc-2//epc17-1/14s14p14d and B3LYP/pc-2//epc-1/14s14p14d levels, respectively, while the uncorrelated densities are derived at the B3LYP/pc-2//no-epc/14s14p14d and B3LYP/pc-2//no-epc/14s14p14d levels, respectively (for more details see Appendix B). The reference densities for the model are obtained from the computed exact wave function, whereas the uncorrelated densities are derived at the MCHF/[7s7p7d/7s7p7d] level. In the case of the model, all ρ_e are isotropic and the center of the coordinate system is placed at the joint center of the traps. For the real molecules, ρ_e are anisotropic and the axis used to depict the densities goes through the maximum of $\rho_{p/\mu}$ and the clamped carbon nucleus where the latter is located at the center of the coordinate system.

$F[\rho_e, \rho_{p/\mu}]$ is the Hohenberg-Kohn universal functional of the model which is a functional of ρ_e and $\rho_{p/\mu}$, independent from v_e^{ext} and $v_{p/\mu}^{\text{ext}}$. Assuming there is a noninteracting two-particle reference KS system for the model, reproducing the exact one-particle densities, the universal functional may be rewritten as follows:

$$\begin{aligned} F[\rho_e, \rho_{p/\mu}] &= T_e^s[\rho_e] + T_{p/\mu}^s[\rho_{p/\mu}] + J_{e-(p/\mu)}[\rho_e, \rho_{p/\mu}] \\ &\quad + E_{e(p/\mu)c}[\rho_e, \rho_{p/\mu}], \\ E_{e(p/\mu)c}[\rho_e, \rho_{p/\mu}] &= (T_e[\rho_e, \rho_{p/\mu}] - T_e^s[\rho_e]) + (T_{p/\mu}[\rho_e, \rho_{p/\mu}] \\ &\quad - T_{p/\mu}^s[\rho_{p/\mu}]) + (V_{e-(p/\mu)}[\rho_e, \rho_{p/\mu}] \\ &\quad - J_{e-(p/\mu)}[\rho_e, \rho_{p/\mu}]). \end{aligned} \quad (4)$$

In these equations $T_e^s[\rho_e] = (-1/2)\langle \phi_e^{\text{KS}} | \nabla_e^2 | \phi_e^{\text{KS}} \rangle$ and $T_{p/\mu}^s[\rho_{p/\mu}] = (-1/2m_{p/\mu})\langle \phi_{p/\mu}^{\text{KS}} | \nabla_{p/\mu}^2 | \phi_{p/\mu}^{\text{KS}} \rangle$ are the KS noninteracting kinetic energies of the electron and the proton/muon while $J_{e-(p/\mu)}[\rho_e, \rho_{p/\mu}] = -\int d\vec{r}_e \int d\vec{r}_{p/\mu} \frac{\rho_e(\vec{r}_e)\rho_{p/\mu}(\vec{r}_{p/\mu})}{|\vec{r}_e - \vec{r}_{p/\mu}|}$ is the classical Coulomb interaction energy, sometimes also called the Hartree term. Neglecting the spin, the KS wave function of the model is the product of the KS spatial orbitals: $\Psi_{\text{KS}}(\vec{r}_e, \vec{r}_{p/\mu}) = \phi_e^{\text{KS}}(\vec{r}_e)\phi_{p/\mu}^{\text{KS}}(\vec{r}_{p/\mu})$, where: $\rho_e = |\phi_e^{\text{KS}}|^2$ and $\rho_{p/\mu} = |\phi_{p/\mu}^{\text{KS}}|^2$ are the one-particle densities of the model. The only unknown is the functional

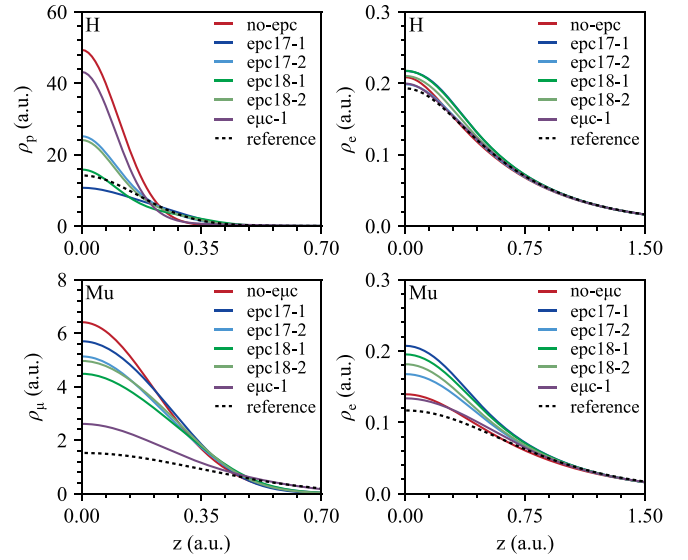


FIG. 3. 1D slices of the reference, functional- and MCHF-derived ρ_e and $\rho_{p/\mu}$ for H/Mu-DHT. Since all the one-particle densities are isotropic, the direction of the z axis is arbitrary and the center of the coordinate system is placed at the joint center of the double harmonic traps.

form of the electron-proton/muon correlation functional, $E_{e(p/\mu)c}[\rho_e, \rho_{p/\mu}]$. Upon the variation of the energy functional, Eq. (3), with respect to the KS spatial orbitals, the following set of coupled KS equations are derived:

$$\begin{aligned} \left(-\frac{1}{2}\nabla_e^2 + v_e^{\text{KS}}(\vec{r}_e)\right)\phi_e^{\text{KS}}(\vec{r}_e) &= \varepsilon_e^{\text{KS}}\phi_e^{\text{KS}}(\vec{r}_e) \\ \left(-\frac{1}{2m_{p/\mu}}\nabla_{p/\mu}^2 + v_{p/\mu}^{\text{KS}}(\vec{r}_{p/\mu})\right)\phi_{p/\mu}^{\text{KS}}(\vec{r}_{p/\mu}) &= \varepsilon_{p/\mu}^{\text{KS}}\phi_{p/\mu}^{\text{KS}}(\vec{r}_{p/\mu}), \\ v_e^{\text{KS}}(\vec{r}_e) &= v_e^{\text{ext}}(\vec{r}_e) + v_e^J(\vec{r}_e) + v_e^{e(p/\mu)c}(\vec{r}_e) \\ v_{p/\mu}^{\text{KS}}(\vec{r}_{p/\mu}) &= v_{p/\mu}^{\text{ext}}(\vec{r}_{p/\mu}) + v_{p/\mu}^J(\vec{r}_{p/\mu}) + v_{p/\mu}^{e(p/\mu)c}(\vec{r}_{p/\mu}). \end{aligned} \quad (5)$$

In these equations, $v_e^{\text{KS}}(\vec{r}_e)$ and $v_{p/\mu}^{\text{KS}}(\vec{r}_{p/\mu})$ are the effective KS electronic and protonic/muonic potentials, respectively. Their components, apart from the external potentials, are $v_e^J(\vec{r}_e) = \frac{\delta J_{e-(p/\mu)}}{\delta \rho_e} = -\int d\vec{r}_{p/\mu} \frac{\rho_{p/\mu}(\vec{r}_{p/\mu})}{|\vec{r}_e - \vec{r}_{p/\mu}|}$ and $v_{p/\mu}^J(\vec{r}_{p/\mu}) = \frac{\delta J_{e-(p/\mu)}}{\delta \rho_{p/\mu}} = -\int d\vec{r}_e \frac{\rho_e(\vec{r}_e)}{|\vec{r}_e - \vec{r}_{p/\mu}|}$, as the potentials emerging from the Hartree term, and, $v_e^{e(p/\mu)c}(\vec{r}_e) = \frac{\delta E_{e(p/\mu)c}}{\delta \rho_e}$ and $v_{p/\mu}^{e(p/\mu)c}(\vec{r}_{p/\mu}) = \frac{\delta E_{e(p/\mu)c}}{\delta \rho_{p/\mu}}$, as the electronic and protonic/muonic correlation potentials, respectively.

Since the exact functional form of $E_{e(p/\mu)c}[\rho_e, \rho_{p/\mu}]$ is unknown, in order to start solving the KS equations, an approximate functional form must be used to deduce the corresponding correlation potentials. Such approximate functionals are considered in the next section, but since $\Psi_{\text{exact}}(\vec{r}_e, \vec{r}_{p/\mu})$ and the concomitant exact ρ_e and $\rho_{p/\mu}$ are known, depicted in Fig. 3, the exact correlations potentials are also deducible from an inversion process similar to that employed previously in the case of the harmonium model [203,207,208]. The relevant expressions, derived from the coupled KS equations, are

TABLE I. The exact/reference and approximate KS energy components computed for H/Mu-DHT (for the definition of each term see Sec. II C). The entry denoted as reference contains the exact results while the others are obtained with and without the considered electron-proton/muon correlation functionals.

Method	E_{ground}	T_e^s	$\langle v_e^{\text{ext}} \rangle$	$T_{p/\mu}^s$	$\langle v_{p/\mu}^{\text{ext}} \rangle$	$J_{e-(p/\mu)}$	$E_{e(p/\mu)c}$	$\varepsilon_e^{\text{KS}}$	$\varepsilon_{p/\mu}^{\text{KS}}$
H									
no-epc/MCHF	-0.4628	0.4561	0.0002	0.0171	0.0033	-0.9393	0.0000	-0.48	-0.919
epc17-1	-0.5112	0.4928	0.0001	0.0083	0.0075	-0.9564	-0.0636	-0.50	-0.978
epc17-2	-0.4874	0.4606	0.0002	0.0094	0.0062	-0.9323	-0.0314	-0.49	-0.932
epc18-1	-0.4971	0.4928	0.0001	0.0074	0.0085	-0.9527	-0.0532	-0.50	-0.959
epc18-2	-0.4829	0.4751	0.0002	0.0092	0.0066	-0.9443	-0.0297	-0.49	-0.939
e μ c-1	-0.4786	0.4646	0.0002	0.0121	0.0077	-0.9319	-0.0314	-0.49	-0.922
Reference	-0.4846	0.4649	0.0002	0.0075	0.0075	-0.9315	-0.0331	-0.49	0.015
Mu									
no-e μ c/MCHF	-0.4078	0.3892	0.0007	0.0383	0.0059	-0.8419	0.0000	-0.45	-0.798
epc17-1	-0.4690	0.4882	0.0006	0.0415	0.0055	-0.9351	-0.0696	-0.50	-0.942
epc17-2	-0.4486	0.4378	0.0007	0.0360	0.0063	-0.8855	-0.0439	-0.48	-0.873
epc18-1	-0.4628	0.4762	0.0006	0.0357	0.0064	-0.9180	-0.0637	-0.50	-0.916
epc18-2	-0.4432	0.4515	0.0006	0.0381	0.0060	-0.8995	-0.0399	-0.48	-0.882
e μ c-1	-0.4547	0.4072	0.0007	0.0213	0.0108	-0.8328	-0.0619	-0.47	-0.821
Reference	-0.4670	0.3944	0.0007	0.0151	0.0149	-0.8035	-0.0885	-0.49	0.030

the following:

$$\begin{aligned}
 v_e^{e(p/\mu)c}(\vec{r}_e) &= \varepsilon_e^{\text{KS}} - v_e^{\text{ext}}(\vec{r}_e) - v_e^J(\vec{r}_e) + \frac{\nabla_e^2 \phi_e^{\text{KS}}(\vec{r}_e)}{2\phi_e^{\text{KS}}(\vec{r}_e)}, \\
 v_{p/\mu}^{e(p/\mu)c}(\vec{r}_{p/\mu}) &= \varepsilon_{p/\mu}^{\text{KS}} - v_{p/\mu}^{\text{ext}}(\vec{r}_{p/\mu}) - v_{p/\mu}^J(\vec{r}_{p/\mu}) \\
 &\quad + \frac{\nabla_{p/\mu}^2 \phi_{p/\mu}^{\text{KS}}(\vec{r}_{p/\mu})}{2m_{p/\mu} \phi_{p/\mu}^{\text{KS}}(\vec{r}_{p/\mu})}. \quad (6)
 \end{aligned}$$

Comparison between the exact and an approximate correlation potential is probably the most stringent quality measure of an approximate functional as also demonstrated in the case of the electronic exchange-correlation functionals [203,207,208,260–267]. Let us now turn to the numerical application of the formalism to the model.

Since $|\phi_e^{\text{KS}}| = \sqrt{\rho_e}$ and $|\phi_{p/\mu}^{\text{KS}}| = \sqrt{\rho_{p/\mu}}$, apart from the phase, ϕ_e^{KS} and $\phi_{p/\mu}^{\text{KS}}$ are available, and the numerical values of all energy components except for $E_{e(p/\mu)c}$, namely, T_e^s , $T_{p/\mu}^s$, $J_{e-(p/\mu)}$, $\langle v_e^{\text{ext}} \rangle$, $\langle v_{p/\mu}^{\text{ext}} \rangle$, are easily computable. The eigenvalue problems of the Hamiltonians given in Eq. (2) are solved exactly and $E_{\text{exact}} = E_R + E_r$ is numerically known, thus, $E_{e(p/\mu)c}$ is computed as follows: $E_{e(p/\mu)c} = E_{\text{exact}} - (T_e^s + T_{p/\mu}^s + J_{e-(p/\mu)} + \langle v_e^{\text{ext}} \rangle + \langle v_{p/\mu}^{\text{ext}} \rangle)$. Alternatively, since the expectation values of the operators composing the original Hamiltonian, Eq. (1), are all known, it is feasible to compute $E_{e(p/\mu)c}$ directly using Eq. (4); both methods yield the same numerical value.

All total energies and their components are gathered for H/Mu-DHT in Table I. Most notable is the twice larger $E_{e\mu c}$ in comparison to E_{epc} , consistent with the known fact that the correlation energy is inversely related to the mass of the PCP. In order to derive the KS orbital energies, $\varepsilon_e^{\text{KS}}$ and $\varepsilon_{p/\mu}^{\text{KS}}$, the known trick of imposing the following asymptotic conditions was used: $\lim_{|\vec{r}_e| \rightarrow \infty} v_e^{e(p/\mu)c}(\vec{r}_e) \rightarrow 0$ and $\lim_{|\vec{r}_{p/\mu}| \rightarrow \infty} v_{p/\mu}^{e(p/\mu)c}(\vec{r}_{p/\mu}) \rightarrow 0$ (for more details see [203,207,208]), and the numerical results are also given in

Table I. Interestingly, the values of $\varepsilon_e^{\text{KS}}$ in both systems are very near the ground state energy of the free hydrogen atom, ~ -0.5 , while those of $\varepsilon_{p/\mu}^{\text{KS}}$ are practically equal to the zero-point energy of the harmonic traps, $\varepsilon_p^{\text{KS}} \sim \frac{3}{2}\omega_{\text{proton}} = 0.015$ and $\varepsilon_\mu^{\text{KS}} \sim \frac{3}{2}\omega_{\text{muon}} = 0.03$. To have a ‘‘local’’ picture of the role of the correlations, Fig. 4 depicts v_e^{KS} and $v_{p/\mu}^{\text{KS}}$ as well as their components individually as introduced in Eq. (5). It is evident that the role of the protonic/muonic correlation potentials is pivotal, eliminating the Hartree part of the po-

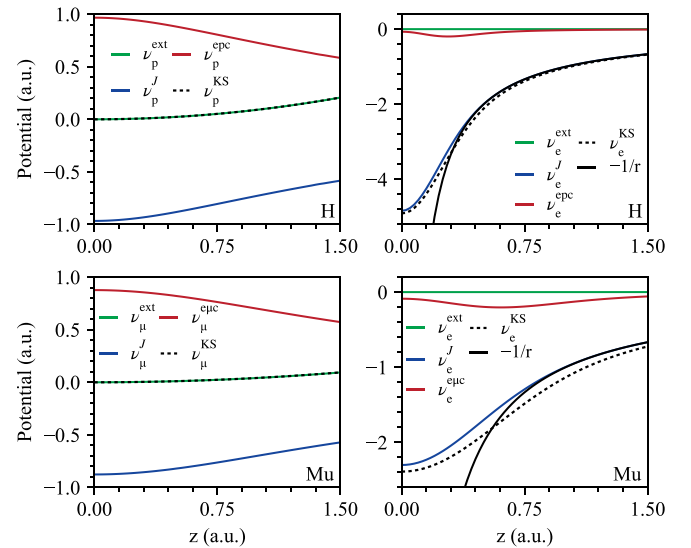


FIG. 4. The reference v_e^{KS} and $v_{p/\mu}^{\text{KS}}$ and their components v_e^{ext} , v_e^J , $v_e^{e(p/\mu)c}$, and $v_{p/\mu}^{\text{ext}}$, $v_{p/\mu}^J$, $v_{p/\mu}^{e(p/\mu)c}$, respectively, for H/Mu-DHT [see Eq. (5) for more details]. The Coulomb’s law, the solid black line, is also given in the right-hand panels for comparison. Since all the potentials are isotropic, the direction of the z axis is arbitrary and the center of the coordinate system is placed at the joint center of the double harmonic traps.

tential, $v_{p/\mu}^{e(p/\mu)c} \approx -v_{p/\mu}^J$. Thus, to a very good approximation: $v_{p/\mu}^{KS} \approx v_{p/\mu}^{ext}$, which explains why the numerical values of $\varepsilon_{p/\mu}^{KS}$ are equal to the zero-point energy of the traps. In contrast, the contribution of $v_e^{e(p/\mu)c}$ is marginal in shaping v_e^{KS} and only modifies the dominant contribution of v_e^J slightly, thus, to a good approximation: $v_e^{KS} \approx v_e^J$. As is evident from the figure, upon taking some distance from the joint center of the traps the Hartree potential quickly approaches the Coulomb law: $v_e^J \sim -\frac{1}{r}$, and this may explain the origin of the numerical values of ε_e^{KS} .

Based on these observations, we conclude that the model is capable of providing a clear understanding of the roles of the correlation potentials, however, as is discussed in the next section, the reproduction of these potentials through applying approximate functionals to the coupled KS equations is not an easy task.

III. ASSESSING THE QUALITY OF THE LOCAL ELECTRON-PROTON/MUON CORRELATION FUNCTIONALS

A. Applying approximate correlation functionals to the model

In this section, some recently developed local electron-proton/muon correlation functionals are applied to the KS system of the model through the solution of the coupled KS equations. The resulting numerical data are compared to the reference solutions obtained in the previous section. Let us first briefly review the studied functionals and some computational details regarding the implementation of the coupled KS equations.

There were several proposed electron-proton correlation functionals before the introduction of the epc series [92–94,97,101,268]. However, to the best of our knowledge, none has systematically been evaluated through the standard self-consistent field (SCF) solution of the coupled KS equations on benchmark sets of molecules or crystals. Thus, in the present study we choose the local electron-proton correlation functionals from the epc series, namely, epc17-1 [104], epc17-2 [157], epc18-1 and epc18-2 [105], as well as euc-1, as the electron-muon correlation functional [108]; the functional forms are given in Appendix C. All these functionals have been evaluated carefully in previous benchmark computational studies, and all are capable of remedying the overlocalization of the uncorrelated $\rho_{p/\mu}$.

In order to apply the functionals to the model, we modified our in-house version of the NEO code [36,108,269], implemented in the GAMESS quantum computational package [270], to include external harmonic potentials. The coupled KS equations were solved by expanding KS spatial orbitals in the previously described [7s7p7d/7s7p7d] basis set. For comparison purposes, the coupled KS equations were also solved without any correlation functional, abbreviated as the no-e(p/μ)c levels. Since there is no electron-electron correlation potential in the KS equations, these are practically equivalent to the MCHF/[7s7p7d/7s7p7d] computational level. The final numerical results are gathered in Table I and the resulting ρ_e and $\rho_{p/\mu}$ are depicted in Fig. 3 while the derived v_e^{KS} and $v_{p/\mu}^{KS}$ as well as their components are depicted in Figs. 5–7.

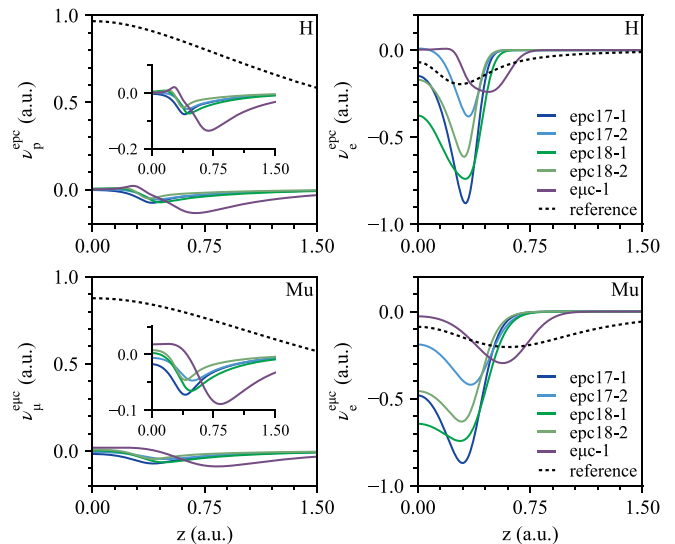


FIG. 5. The reference and functional-derived correlation potentials for H/Mu-DHT. The reference correlation potentials are the exact results, depicted previously in Fig. 4, while the others have been deduced using the considered electron-proton/muon correlation functionals. The potentials deduced for each functional are computed using $\rho_{p/\mu}$ and ρ_e derived from the SCF solution of the coupled KS equations. The insets are zoomed views of the functional-derived potentials. Since all the potentials are isotropic, the direction of the z axis is arbitrary and the center of the coordinate system is placed at the joint center of the double harmonic traps.

Let us first compare the functional-derived ρ_e and $\rho_{p/\mu}$ with the reference densities as one of the basic outputs of the SCF solutions of the coupled KS equations. Since the one-particle densities are isotropic, only a 1D plot of the densities along an arbitrary axis going through the joint centers of the double harmonic traps is given in Fig. 3. In the case of H-DHT, the computed ρ_e with various correlation functionals, even that derived at the no-epc level, are almost superimposable on the reference ρ_e . In contrast, the computed ρ_p is clearly overlocalized at the no-epc level but those derived using the correlation functionals of the epc series to a large extent reduce the overlocalization. Particularly, ρ_p derived from epc17-1 and epc18-1 are almost similar to the reference ρ_p in line with the fact that the numerical values of the parameters of these two functionals were optimized to reproduce the exact ρ_p in molecules [104,105]. The worst result between the functionals is that of euc-1 and this is also understandable since this functional has been primarily designed to cope with the overlocalization of ρ_μ in muonic molecules. In the case of Mu-DHT, the situation is to some extent different, and the computed ρ_e using various functional vary considerably. Oddly, the epc series is acting even worse than the no-euc level when compared to the reference ρ_e and only euc-1, to some extent, is able to reproduce the reference ρ_e . The uncorrelated ρ_μ computed at the no-euc level is evidently overlocalized and all functionals to some extent reduce the overlocalization although euc-1 is clearly superior to the epc series. All these observations are promising and reveal the fact that the correlation functionals overcome the overlocalization of $\rho_{p/\mu}$, as they do in the case of real molecules. Also, we may claim that the

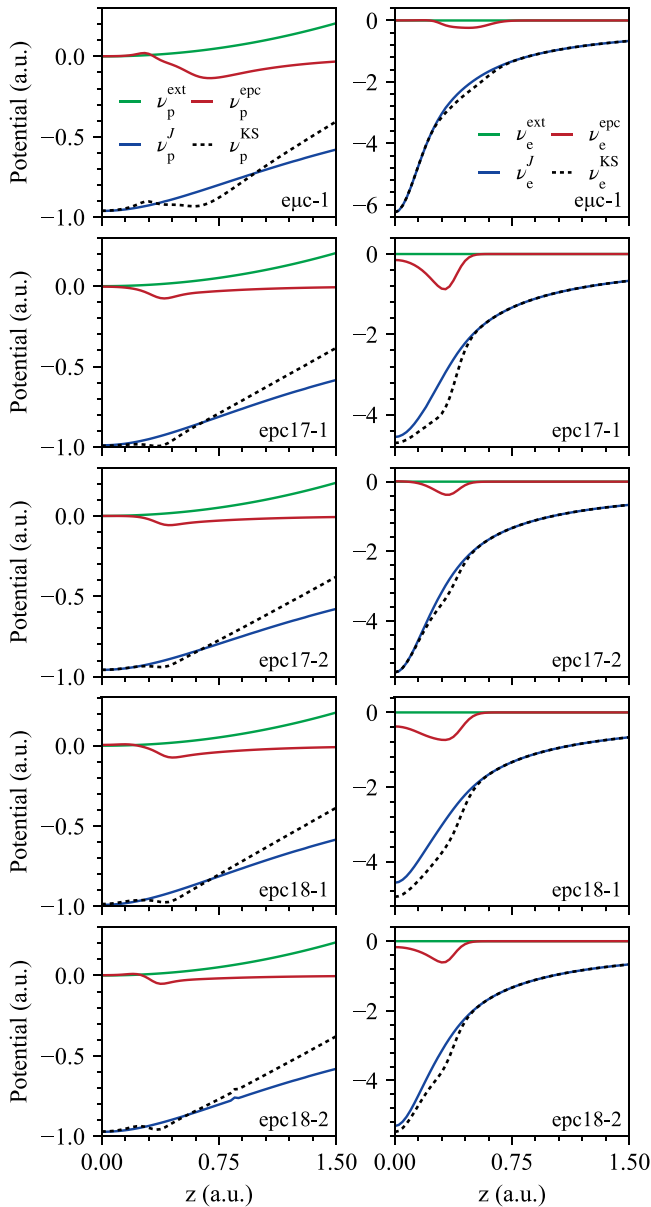


FIG. 6. The functional-derived ν_p^{KS} and ν_e^{KS} , and their components, ν_p^{ext} , ν_p^J , ν_p^{epc} , and ν_e^{ext} , ν_e^J , ν_e^{epc} , respectively, for H-DHT [see Eq. (5) for more details], deduced from the SCF-derived ρ_e and ρ_p . The protonic and electronic potentials are shown in the left- and right-hand panels, respectively. Since all the potentials are isotropic, the direction of the z axis is arbitrary and the center of the coordinate system is placed at the joint center of the double harmonic traps.

model is sensitive enough to differentiate correctly between the functionals and reveal their special m_{PCP} -dependent capabilities.

Now, let us consider the KS energy contributions derived from each functional as given in Table I. The parameters of epc17-2 and epc18-2 were optimized to reproduce the zero-point energy of the proton in molecules thus one expects their performance in reproducing energetics to be superior in the epc series [105,157]. Indeed, both functionals reproduce the reference total energy of H-DHT and its components almost exactly. In contrast, epc17-1 and epc18-1 overestimate the absolute amount of the total energy as well as T_e^s and J_{e-p} as

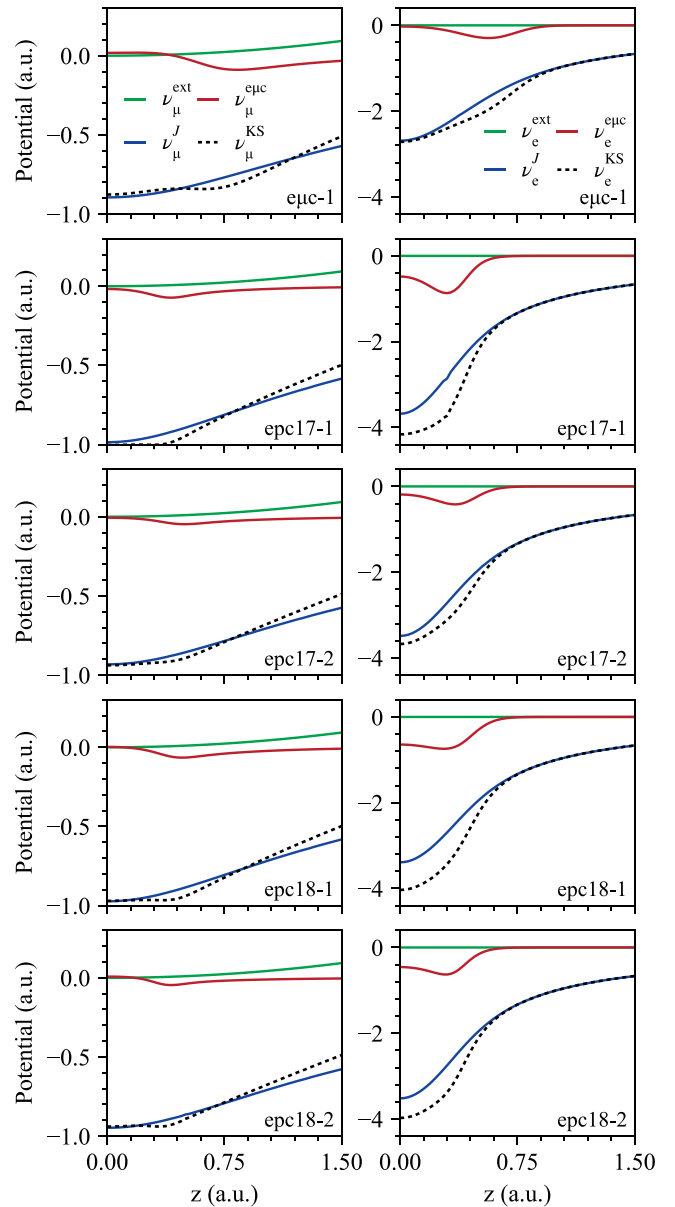


FIG. 7. The functional-derived ν_e^{KS} and ν_μ^{KS} , and their components, ν_e^{ext} , ν_e^J , ν_e^{epc} , and ν_μ^{ext} , ν_μ^J , ν_μ^{epc} , respectively, for Mu-DHT [see Eq. (5) for more details], deduced from the SCF-derived ρ_e and ρ_μ . The muonic and electronic potentials are shown in the left- and right-hand panels, respectively. Since all the potentials are isotropic, the direction of the z axis is arbitrary and the center of the coordinate system is placed at the joint center of the double harmonic traps.

the two major components of the total energy. Interestingly, the performance of euc-1 is much better than epc17-1 and epc18-1, and the only major error of this functional is in the correct reproduction of T_p^s . In line with these observations, epc17-2, epc18-2, and euc-1 are capable of recovering the reference E_{epc} quite precisely. Also, all functionals and even the no-epc level are capable of recovering the reference $\varepsilon_e^{\text{KS}}$, but concomitantly all of them severely underestimate the value of the reference $\varepsilon_p^{\text{KS}}$, ~ 0.015 , predicting large negative values, ~ -0.9 . As will be discussed subsequently in detail, the origin of this failure may be traced to the unsuccessful

reproduction of the reference v_p^{KS} . Let us now turn to Mu-DHT, starting from the unexpected accurate recovery of the total reference energy by epc17-1 and epc18-1. Nevertheless, after an inspection of the energy components, it turns out that this must be due to error cancellations, since none reproduce the reference values of T_e^s and $J_{e-\mu}$ accurately. In contrast, epc17-2 and epc18-2 are not capable of recovering the total reference energy or the components properly. Expectedly, epc-1 outperforms all the other functionals, however, even in this case the recovery of the reference $E_{\text{e}\mu\text{c}}$ is not very accurate. Finally, similar to the case of H-DHT, all functionals are capable of recovering the reference $\varepsilon_e^{\text{KS}}$ but none succeeds in reproducing the value of the reference $\varepsilon_\mu^{\text{KS}}$.

To have a local view on the nature of correlations, Fig. 5 depicts the functional-derived correlation potentials deduced from the SCF-derived ρ_e and $\rho_{p/\mu}$ as well as the reference potentials. Since all potentials are isotropic, only 1D plots along an arbitrary axis going through the joint centers of the double harmonic traps are given in the figure. Figure 5 reveals that v_p^{epc} and $v_\mu^{\text{e}\mu\text{c}}$ deduced from the functionals of the epc series are quite similar and distinct from those deduced from epc-1. The most prominent feature of this figure is the total failure of the functionals to reproduce the reference v_p^{epc} and $v_\mu^{\text{e}\mu\text{c}}$, and none are even remotely similar to the reference potentials. This is a disappointing result but let us stress that the situation is usually no better in the case of many seemingly successful electronic exchange-correlation functionals. This fact has been demonstrated long ago through a similar inversion process applied to the two-electron harmonium and helium atoms [203,207,208,213,260,271]. Accordingly, the reason(s) behind the successful reconstruction of ρ_e and $\rho_{p/\mu}$, and the KS energetics of the considered functionals is not tied to the successful reconstruction of the corresponding correlation potentials (for a relevant discussion, albeit for the electronic exchange-correlation functionals, see Refs. [272,273]). Most observations described above hold in the case of v_e^{epc} and $v_e^{\text{e}\mu\text{c}}$, depicted in Fig. 5, with the major exception of clear similarities between the reference and functional-derived potentials particularly for epc-1 derived potentials. This is a pleasant feature of the studied correlation functions, however, the role of $v_e^{\text{e}(p/\mu)\text{c}}$ on shaping v_e^{KS} is marginal and largely confined to the modification of the dominant v_e^J at small distances (*vide infra*). Thus future efforts to design proper electron-proton/muon functionals should mainly concentrate on the successful reproduction of v_p^{epc} and $v_\mu^{\text{e}\mu\text{c}}$.

Let us now inspect the functional-derived effective potentials and their components, similar to those depicted in Fig. 4 for the reference KS system. Figure 6 depicts the functional-derived v_e^{KS} and $v_{p/\mu}^{\text{KS}}$, and their components, respectively, computed from the SCF-derived ρ_e and ρ_p for H-DHT. Figure 7 depicts the same quantities for Mu-DHT revealing in conjunction with Fig. 6 that the derived v_e^{KS} and $v_{p/\mu}^{\text{KS}}$, and their components, are similar in the considered functionals particularly if only the epc series is taken into account. For all functionals, v_e^{KS} has a minimum at the joint center of the harmonic traps and is almost superimposable on v_e^J with some marginal digressions induced by $v_e^{\text{e}(p/\mu)\text{c}}$. Interestingly, the reference v_e^{KS} depicted in Fig. 4 shares the same features with the functional-derived potentials, and this explains why the reference $\varepsilon_e^{\text{KS}}$ is properly recovered by the used

functionals. In contrast, none of the functional-derived $v_{p/\mu}^{\text{KS}}$ is even remotely similar to the reference potential which as discussed, is practically equal to $v_{p/\mu}^{\text{ext}}$. This observation explains why the functional-derived $\varepsilon_p^{\text{KS}}$ values are severely disparate from those of the reference values, as disclosed previously. The dissimilarity stems from the fact that in contrast to the reference KS system, $v_{p/\mu}^{\text{e}(p/\mu)\text{c}}$ are unable to cancel the effect of $v_{p/\mu}^J$.

We conclude that both epc series and epc-1 are able to remedy the overlocalization of uncorrelated one-proton/muon densities in H/Mu-DHT, respectively. Moreover, they are also generally successful in reproducing the KS energetics and the electronic correlation potentials. Nonetheless, they are especially unable to reproduce the protonic/muonic KS orbital energies as well as the corresponding correlation potentials. Taking the fact that the model contains solely the electron-proton/muon correlation, the mentioned success confirms the capacity of these functionals to cope at least partly with this type of correlation. By the way, the mentioned failures also point to the fact that much room remains to improve the correlation functional design strategies. The model itself may serve as the target system for primary tests of any new electron-proton/muon correlation functional introduced in future studies.

B. Disentangling the density-driven and the intrinsic errors of the functionals

In the previous subsection, the quality of the correlation functionals was evaluated through the results gained from the SCF solution of the KS coupled equations. However, it is well-documented that this procedure is prone to two independent sources of errors [274–276]. One comes from the approximate nature of the functional itself, called intrinsic functional errors, and the other stems from the approximate one-particle densities derived from the SCF procedure, called density-driven errors. In this subsection, we try to disentangle these two errors to access the intrinsic quality of the studied correlation functionals by considering the associated potentials as well as the computed energies.

Figure 8 depicts the functional-derived correlation potentials deduced from the reference $\rho_{p/\mu}$ and ρ_e , respectively. In the case of H-DHT, through comparison with Fig. 5, it becomes evident that for each functional, v_p^{epc} and v_e^{epc} deduced from reference and SCF-derived ρ_p and ρ_e are almost superimposable. The justification is that the reference and the SCF-derived ρ_e of all the studied functionals are almost superimposable, whereas the corresponding ρ_p are quite localized around the joint center of the traps (see Fig. 3). Accordingly, ρ_e has a much more important role in shaping the topographies of v_p^{epc} and v_e^{epc} , and ρ_p only affects the potentials around the joint center of the harmonic traps. The situation is completely different in the case of Mu-DHT as the epc series derived $v_\mu^{\text{e}\mu\text{c}}$ and $v_e^{\text{e}\mu\text{c}}$ vary considerably upon replacing the reference ρ_μ and ρ_e with their SCF-derived counterparts. The justification lies in the pronounced differences between the reference and SCF-derived ρ_e as well as the less localized nature of ρ_μ compared to ρ_p (see Fig. 3). Figure 8 also reveals that the minima of the epc series derived $v_\mu^{\text{e}\mu\text{c}}$ and $v_e^{\text{e}\mu\text{c}}$ are all displaced to the

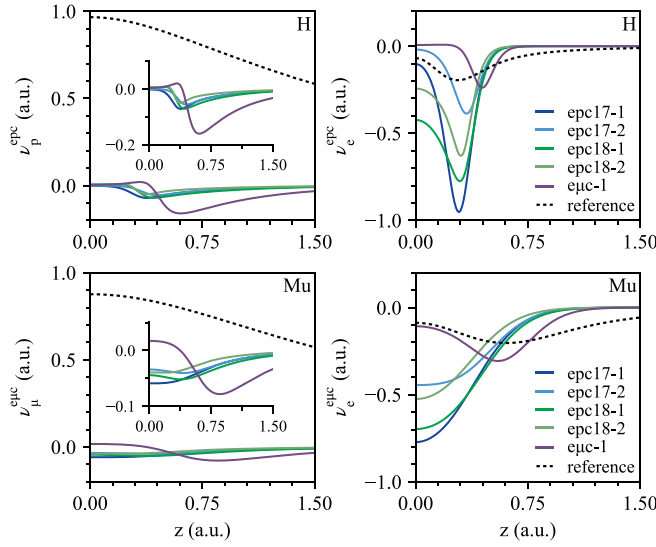


FIG. 8. The reference and functional-derived correlation potentials for H/Mu-DHT. The reference correlation potentials are the exact results, depicted previously in Fig. 4, while the others have been deduced using the considered electron-proton/muon correlation functionals. The potentials deduced for each functional are computed using the reference/exact $\rho_{p/\mu}$ and ρ_e . The insets are zoomed views of the functional-derived potentials. Since all the potentials are isotropic, the direction of the z axis is arbitrary and the center of the coordinate system is placed at the joint center of the double harmonic traps.

joint center of the traps upon using the reference ρ_μ and ρ_e instead of the SCF-derived one-particle densities. Evidently, the lighter Mu-DHT is a more sensitive probe to check the density-dependence of the correlation potentials than H-DHT. Interestingly, in contrast to the v_μ^{epc} and v_e^{epc} derived from the epc series of functionals, those of epc-1 are less sensitive to the replacement of the SCF-derived ρ_μ and ρ_e with the reference densities. One may conclude at this stage that among the considered functionals, epc-1 is least affected by density errors, as far as one is concerned with the correlation potentials.

TABLE II. The functional-derived $E_{e(p/\mu)c}$ computed using the uncorrelated, $E_{e(p/\mu)c}^{\text{no-e}(p/\mu)c}$, the SCF-derived, $E_{e(p/\mu)c}^{\text{SCF}}$, (retrieved from Table I), and the reference, $E_{e(p/\mu)c}^{\text{ref}}$, one-particle densities for H/Mu-DHT. The differences in the last two columns are given in kcal/mol.

Functional	$E_{e(p/\mu)c}^{\text{no-e}(p/\mu)c}$	$E_{e(p/\mu)c}^{\text{SCF}}$	$E_{e(p/\mu)c}^{\text{ref}}$	$E_{e(p/\mu)c}^{\text{no-e}(p/\mu)c} - E_{e(p/\mu)c}^{\text{ref}}$	$E_{e(p/\mu)c}^{\text{SCF}} - E_{e(p/\mu)c}^{\text{ref}}$
H					
epc17-1	-0.0344	-0.0636	-0.0565	13.9	-4.5
epc17-2	-0.0189	-0.0314	-0.0346	9.9	2.0
epc18-1	-0.0208	-0.0532	-0.0427	13.8	-6.6
epc18-2	-0.0140	-0.0297	-0.0293	9.5	-0.3
epc-1	-0.0048	-0.0314	-0.0191	9.0	-7.7
Mu					
epc17-1	-0.0524	-0.0696	-0.0406	-7.4	-18.2
epc17-2	-0.0379	-0.0439	-0.0367	-0.7	-4.5
epc18-1	-0.0469	-0.0637	-0.0461	-0.5	-11.0
epc18-2	-0.0312	-0.0399	-0.0258	-3.4	-8.8
epc-1	-0.0337	-0.0619	-0.0700	22.8	5.1

Table II offers the functional-derived $E_{e(p/\mu)c}$ for H/Mu-DHT computed using the uncorrelated, the SCF-derived (retrieved from Table I) and the reference one-particle densities. Inspection of the last two columns of the table demonstrates that in the case of H-DHT the computed E_{epc} from the epc series of functionals using the SCF-derived ρ_p and ρ_e is much more accurate than those derived using the uncorrelated densities. The same is true about the computed E_{epc} for Mu-DHT using epc-1, however, surprisingly, the epc series of functionals seem to work better when using the uncorrelated ρ_μ and ρ_e . This is probably the result of some type of error cancellation, though it is hard to pinpoint its exact nature. Nevertheless, these observations once again witness the model's capacity to differentiate between the epc series and epc-1 functionals, revealing their system-specific performance. With these results at hand, we may now proceed to compute the density-driven and intrinsic functional errors in total energies.

In order to disentangle the density-driven and intrinsic functional errors of the functionals in reproducing the total energies, the following equation is used where for consistency, the notation is borrowed from the original literature [274–276]:

$$\begin{aligned}
 \Delta E &= \tilde{E}[\tilde{\rho}_e, \tilde{\rho}_{p/\mu}] - E[\rho_e, \rho_{p/\mu}] \\
 &= (\tilde{E}[\tilde{\rho}_e, \tilde{\rho}_{p/\mu}] - \tilde{E}[\rho_e, \rho_{p/\mu}]) \\
 &\quad + (\tilde{E}[\rho_e, \rho_{p/\mu}] - E[\rho_e, \rho_{p/\mu}]) \\
 &= \Delta E_D + \Delta E_F.
 \end{aligned} \tag{7}$$

In this equation, tildes are used to denote the SCF-derived total energies and the one-particle densities while those without tildes are the references; ΔE_D is the density-driven error and ΔE_F is the intrinsic error of a functional in reproducing the total exact energy. Table III offers ΔE , ΔE_D and ΔE_F for the five considered functionals using the data from Tables I and II. In the case of H-DHT, ΔE_F is the dominant error for epc17-1 and epc18-1 while for the remaining functionals and at the no-epc level, the values of ΔE_D are comparable to those of ΔE_F . As discussed previously, epc17-2 and epc18-2 are capable of reproducing the KS energetics of H-DHT accurately

TABLE III. The density-driven, ΔE_D , and the intrinsic, ΔE_F , and the total energy, ΔE , errors of the considered functionals computed for H/Mu-DHT [see Eq. (7) for the definitions]. The numbers are given in kcal/mol.

Method	ΔE_D	ΔE_F	ΔE
H			
no-epc	-7.1	20.7	13.7
epc17-1	-2.0	-14.7	-16.7
epc17-2	-0.8	-1.0	-1.8
epc18-1	-1.9	-6.1	-7.9
epc18-2	-1.4	2.4	1.0
epc-1	-5.1	8.8	3.7
Mu			
no-epc	-18.4	55.5	37.1
epc17-1	-31.3	30.0	-1.3
epc17-2	-21.0	32.5	11.5
epc18-1	-24.0	26.6	2.6
epc18-2	-24.5	39.4	14.9
epc-1	-4.0	11.6	7.6

and while their overall ΔE is small compared to the other considered functionals, ΔE_D seems to have a non-negligible contribution to this success. In the case of Mu-DHT, ΔE_D is also a major source of error for all the considered functionals except for epc-1, which as discussed is capable of reproducing KS energetics accurately, although even for this functional its contribution is not negligible. Interestingly, in most cases, the signs of ΔE_D and ΔE_F are different and ΔE_D masks the larger intrinsic errors of the considered functionals. We conclude that the success of the considered correlation functionals to reproduce KS energetics is not solely revealing their intrinsic performance, but partly it is the result of the density-driven errors.

IV. CONCLUSIONS AND PROSPECTS

The electron-PCP correlation functional design is a vital part of MCDFT, however, in contrast to eDFT [277–287], based on the number of currently available functionals and the used design strategies, it is a much less developed research area. Particularly entertaining is the accessibility to few-body systems containing solely electron-PCP correlation to calibrate the performance of the newly proposed correlation functionals. The two-particle electron-PCP system within the double harmonic trap, proposed in the present study, is the first step in this direction. Notwithstanding, by adding more particles (electrons and/or PCPs) to the model, one may consider the interplay between various types of correlations, i.e., electron-electron, electron-PCP and PCP-PCP. Also, a more comprehensive study of the model itself in a larger domain of the parameters namely, PCP’s mass and the frequency of oscillation, may widen its application beyond protonic and muonic systems and the usual ambient conditions. Another interesting possibility is the application of such simple model systems to gain insight into the design of efficient electron-PCP correlation functionals. As the present study demonstrates, the currently available local electron-proton/muon functionals, with all their achievements, yet have clear weaknesses like

the inability to yield correct protonic/muonic correlation potentials and corresponding orbital energies. Even more, part of their success in predicting correct energetics seems to be the result of the density-driven errors that mask the intrinsic shortcomings of the used functionals. All these point to the fact that much remains to be done in this research area.

ACKNOWLEDGMENTS

S.S. would like to acknowledge the generous access to the computational resources of SARMAD Cluster at Shahid Beheshti University.

APPENDIX A: THE BASIS SET DESIGN FOR THE H/MU-DHT

The uncontracted [7s7p7d/7s7p7d] Gaussian basis set was designed as follows. The exponents of the Gaussian functions were derived through a nonlinear energy optimization at the MCHF/[7s/7s] level and then used without any modification also for the p- and d-type Gaussian functions in the [7s7p7d/7s7p7d] basis set. Two series of exponents were derived, one for the proton’s mass and the other for the muon’s mass within the corresponding frequencies of oscillation, all given in Table IV. This basis set is also used without further modifications to solve the MCKS equations for the model.

APPENDIX B: THE COMPUTATIONAL PROCEDURE OF DEDUCING THE ONE-PARTICLE DENSITIES OF HCN AND MuCN

In the case of HCN and MuCN, since we do not have access to the exact ground state wave functions, the reference $\rho_{p/\mu}$ was derived by employing the double-adiabatic approximation [108,288]. Within the context of this approximation, the proton/muon experiences an effective field produced by electrons and the clamped carbon and nitrogen nuclei. The resulting single-particle Schrödinger equation is solved using the generalized Numerov method [289], and

TABLE IV. The exponents of the s-, p- and d-type Gaussian functions in the [7s7p7d/7s7p7d] basis set.

Exponent	Electron	Proton/Muon
H		
1	15.3638	22.5435
2	4.6647	13.6540
3	0.6693	6.9399
4	0.0573	5.7960
5	1.6563	4.1400
6	0.1286	2.0700
7	0.2893	1.0350
Mu		
1	7.2212	15.8560
2	3.2589	10.4040
3	0.6472	7.0649
4	0.0574	5.2960
5	1.4523	4.1400
6	0.1287	2.0700
7	0.2879	1.0350

the derived one-proton/muon wave function was then squared to yield the reference $\rho_{p/\mu}$. To construct the effective potential, the electronic Schrödinger equation was first solved at the B3LYP/pc-2 level [290,291], for the fixed equilibrium arrangement of the clamped carbon and nitrogen nuclei, while the clamped proton was placed at various points of a 3D cubic grid (for the grid details see [108]). The uncorrelated $\rho_{p/\mu}$ was obtained at the B3LYP/pc-2//no-epc/14s14p14d and B3LYP/pc-2//no-epc/14s14p14d levels, respectively. Note that in this notation no-e(p/μ)c implies that no electron-proton/muon correlation functional is used in the MCKS equations while [14s14p14d] is the protonic/muonic basis set used to expand the protonic/muonic KS spatial orbital (for the basis set details see [108]). The reference ρ_e for XCN species were computed at the B3LYP/

pc-2//epc17-1/14s14p14d and B3LYP/pc-2//epc-1/14s14p14d levels wherein epc17-1 and epc-1 are the electron-proton/muon correlation functionals [104,108], while the uncorrelated ρ_e were derived at the B3LYP/pc-2//no-epc/14s14p14d and B3LYP/pc-2//no-epc/14s14p14d levels.

APPENDIX C: THE EXPLICIT FORMS OF THE CONSIDERED FUNCTIONALS

The used functional forms are given below for comparison:

$$E_{\text{epc17}}[\rho_e, \rho_p] = - \int d\vec{r} \frac{\rho_e(\vec{r}_e)\rho_p(\vec{r}_p)}{a - b(\rho_e(\vec{r}_e)\rho_p(\vec{r}_p))^{1/2} + c\rho_e(\vec{r}_e)\rho_p(\vec{r}_p)},$$

$$E_{\text{epc18}}[\rho_e, \rho_p] = - \int d\vec{r} \frac{\rho_e(\vec{r}_e)\rho_p(\vec{r}_p)}{a' - b'(\rho_e(\vec{r}_e))^{1/3} + \rho_p(\vec{r}_p)^{1/3} + c'(\rho_e(\vec{r}_e))^{1/3} + \rho_p(\vec{r}_p)^{1/3}}^6,$$

$$E_{\text{epc-1}}[\rho_e^\alpha, \rho_e^\beta, \rho_\mu] = - \int d\vec{r} \frac{2\rho_e^\alpha(\vec{r}_e)\rho_\mu(\vec{r}_\mu) - \rho_e^\alpha(\vec{r}_e)\rho_\mu(\vec{r}_\mu)^{3/2}}{1 + 8\rho_e^\alpha(\vec{r}_e)\rho_\mu(\vec{r}_\mu) + 4\rho_e^\alpha(\vec{r}_e)\rho_\mu(\vec{r}_\mu)^{3/2}} + \frac{2\rho_e^\beta(\vec{r}_e)\rho_\mu(\vec{r}_\mu) - \rho_e^\beta(\vec{r}_e)\rho_\mu(\vec{r}_\mu)^{3/2}}{1 + 8\rho_e^\beta(\vec{r}_e)\rho_\mu(\vec{r}_\mu) + 4\rho_e^\beta(\vec{r}_e)\rho_\mu(\vec{r}_\mu)^{3/2}}. \quad (\text{C1})$$

In these expressions, $\int d\vec{r} \equiv \int d\vec{r}_e \int d\vec{r}_{p/\mu} \delta(\vec{r}_e - \vec{r}_{p/\mu})$, and $\rho_e = \rho_e^\alpha + \rho_e^\beta$ where ρ_e^α and ρ_e^β stand for the spin-up and spin-down electron densities, respectively. The constants in the epc series have been derived through regression procedures: $a = 2.35$, $b = 2.4$, $c = 3.2$ for epc17-1 [104], $a = 2.35$, $b = 2.4$, $c = 6.6$ for epc17-2 [157], $a' = 1.8$, $b' = 0.1$, $c' = 0.03$ for epc18-1 [105], and $a' = 3.9$, $b' = 0.5$, $c' = 0.06$ for epc18-2 [105]. Also, it is noteworthy that the kernel of

epc-1 functional for the closed-shell case, where $\rho_e^\alpha = \rho_e^\beta = \frac{\rho_e}{2}$, reduces to the following form [108]:

$$E_{\text{epc-1}}[\rho_e, \rho_\mu] = - \int d\vec{r} \frac{2\rho_e(\vec{r}_e)\rho_\mu(\vec{r}_\mu) - \rho_e(\vec{r}_e)\rho_\mu(\vec{r}_\mu)^{3/2}}{1 + 4\rho_e(\vec{r}_e)\rho_\mu(\vec{r}_\mu) + 2\rho_e(\vec{r}_e)\rho_\mu(\vec{r}_\mu)^{3/2}}. \quad (\text{C2})$$

- [1] F. Pavošević, T. Culpitt, and S. Hammes-Schiffer, Multicomponent quantum chemistry: Integrating electronic and nuclear quantum effects via the nuclear–electronic orbital method, *Chem. Rev.* **120**, 4222 (2020).
- [2] H. J. Ache, Chemistry of the positron and of positronium, *Angew. Chem. Int. Ed.* **11**, 179 (1972).
- [3] M. J. Puska and R. M. Nieminen, Theory of positrons in solids and on solid surfaces, *Rev. Mod. Phys.* **66**, 841 (1994).
- [4] Y. C. Jean, P. E. Mallon, and D. M. Schrader, *Principles and Applications of Positron and Positronium Chemistry* (World Scientific, Singapore, 2003).
- [5] D. L. Bailey, D. W. Townsend, P. E. Valk, and M. N. Maisey, *Positron Emission Tomography: Basic Sciences* (Springer-Verlag, London, 2005).
- [6] G. F. Gribakin, J. A. Young, and C. M. Surko, Positron-molecule interactions: Resonant attachment, annihilation, and bound states, *Rev. Mod. Phys.* **82**, 2557 (2010).
- [7] F. Tuomisto and I. Makkonen, Defect identification in semiconductors with positron annihilation: Experiment and theory, *Rev. Mod. Phys.* **85**, 1583 (2013).
- [8] M. Emami-Razavi and J. W. Darewych, Review of experimental and theoretical research on positronium ions and molecules, *Eur. Phys. J. D* **75**, 188 (2021).
- [9] B. D. Patterson, Muonium states in semiconductors, *Rev. Mod. Phys.* **60**, 69 (1988).
- [10] V. G. Storchak and N. V. Prokof'ev, Quantum diffusion of muons and muonium atoms in solids, *Rev. Mod. Phys.* **70**, 929 (1998).
- [11] S. J. Blundell, Spin-polarized muons in condensed matter physics, *Contemp. Phys.* **40**, 175 (1999).
- [12] K. Nagamine, *Introductory Muon Science* (Cambridge University Press, Cambridge, 2003).
- [13] S. J. Blundell, Muon-spin rotation studies of electronic properties of molecular conductors and superconductors, *Chem. Rev.* **104**, 5717 (2004).
- [14] N. J. Clayden, Muons in chemistry, *Phys. Scr.* **88**, 068507 (2013).
- [15] A. D. Hillier, S. J. Blundell, I. McKenzie, I. Umegaki, L. Shu, J. A. Wright, T. Prokscha, F. Bert, K. Shimomura, A. Berlie, H. Alberto, and I. Watanabe, Muon spin spectroscopy, *Nat. Rev. Methods Primers* **2**, 1 (2022).
- [16] I. L. Thomas, The protonic structure of methane, ammonia, water, and hydrogen fluoride, *Chem. Phys. Lett.* **3**, 705 (1969).
- [17] I. L. Thomas, Protonic structure of molecules. I. Ammonia molecules, *Phys. Rev.* **185**, 90 (1969).
- [18] I. L. Thomas, Selection rules and the protonic spectrum of molecules, *Phys. Rev. A* **2**, 72 (1970).

- [19] B. A. Pettitt, Hartree-Fock theory of proton states in hydrides, *Chem. Phys. Lett.* **130**, 399 (1986).
- [20] B. A. Pettitt and W. Danchura, Self-consistent field proton densities in XH_4 molecules, *J. Phys. B: Atom. Mol. Phys.* **20**, 1899 (1987).
- [21] M. Tachikawa, K. Mori, H. Nakai, and K. Iguchi, An extension of ab initio molecular orbital theory to nuclear motion, *Chem. Phys. Lett.* **290**, 437 (1998).
- [22] M. Tachikawa, K. Mori, K. Suzuki, and K. Iguchi, Full variational molecular orbital method: Application to the positron-molecule complexes, *Int. J. Quantum Chem.* **70**, 491 (1998).
- [23] Y. Shigeta, Y. Ozaki, K. Kodama, H. Nagao, H. Kawabe, and K. Nishikawa, Nonadiabatic molecular theory and its application. II. Water molecule, *Int. J. Quantum Chem.* **69**, 629 (1998).
- [24] Y. Shigeta, H. Takahashi, S. Yamanaka, M. Mitani, H. Nagao, and K. Yamaguchi, Density functional theory without the Born–Oppenheimer approximation and its application, *Int. J. Quantum Chem.* **70**, 659 (1998).
- [25] H. Nakai, Nuclear orbital plus molecular orbital theory: Simultaneous determination of nuclear and electronic wave functions without Born–Oppenheimer approximation, *Int. J. Quantum Chem.* **107**, 2849 (2007).
- [26] S. A. González, N. F. Aguirre, and A. Reyes, Theoretical investigation of isotope effects: The any-particle molecular orbital code, *Int. J. Quantum Chem.* **108**, 1742 (2008).
- [27] T. Ishimoto, M. Tachikawa, and U. Nagashima, Review of multicomponent molecular orbital method for direct treatment of nuclear quantum effect, *Int. J. Quantum Chem.* **109**, 2677 (2009).
- [28] R. Flores-Moreno, E. Posada, F. Moncada, J. Romero, J. Charry, M. Díaz-Tinoco, S. A. González, N. F. Aguirre, and A. Reyes, LOWDIN: The any particle molecular orbital code, *Int. J. Quantum Chem.* **114**, 50 (2014).
- [29] A. Reyes, F. Moncada, and J. Charry, The any particle molecular orbital approach: A short review of the theory and applications, *Int. J. Quantum Chem.* **119**, e25705 (2019).
- [30] J. M. Rodas, J. F. Galindo, A. E. Roitberg, and A. Reyes, The any particle molecular orbital/molecular mechanics approach, *J. Mol. Model.* **25**, 316 (2019).
- [31] S. Hammes-Schiffer, Nuclear–electronic orbital methods: Foundations and prospects, *J. Chem. Phys.* **155**, 030901 (2021).
- [32] T. Helgaker, P. Jørgensen, and J. Olsen, *Molecular Electronic-Structure Theory* (John Wiley & Sons, Ltd, Chichester, UK, 2000).
- [33] P. Fulde, *Correlated Electrons in Quantum Matter*, illustrated edition ed. (World Scientific, Singapore; Hackensack, NJ, 2012).
- [34] P. Cassam-Chenai, B. Suo, and W. Liu, Decoupling electrons and nuclei without the Born–Oppenheimer approximation: The electron-nucleus mean-field configuration-interaction method, *Phys. Rev. A* **92**, 012502 (2015).
- [35] P. Cassam-Chenai, B. Suo, and W. Liu, A quantum chemical definition of electron–nucleus correlation, *Theor. Chem. Acc.* **136**, 52 (2017).
- [36] S. P. Webb, T. Iordanov, and S. Hammes-Schiffer, Multiconfigurational nuclear-electronic orbital approach: Incorporation of nuclear quantum effects in electronic structure calculations, *J. Chem. Phys.* **117**, 4106 (2002).
- [37] C. Swalina, M. V. Pak, A. Chakraborty, and S. Hammes-Schiffer, Explicit dynamical electron-proton correlation in the nuclear-electronic orbital framework, *J. Phys. Chem. A* **110**, 9983 (2006).
- [38] A. Chakraborty, M. V. Pak, and S. Hammes-Schiffer, Inclusion of explicit electron-proton correlation in the nuclear-electronic orbital approach using Gaussian-type geminal functions, *J. Chem. Phys.* **129**, 014101 (2008).
- [39] P. E. Adamson, X. F. Duan, L. W. Burggraf, M. V. Pak, C. Swalina, and S. Hammes-Schiffer, Modeling positrons in molecular electronic structure calculations with the nuclear-electronic orbital method, *J. Phys. Chem. A* **112**, 1346 (2008).
- [40] A. Chakraborty and S. Hammes-Schiffer, Density matrix formulation of the nuclear-electronic orbital approach with explicit electron-proton correlation, *J. Chem. Phys.* **129**, 204101 (2008).
- [41] M. V. Pak, A. Chakraborty, and S. Hammes-Schiffer, Calculation of the positron annihilation rate in PsH with the positronic extension of the explicitly correlated nuclear-electronic orbital method, *J. Phys. Chem. A* **113**, 4004 (2009).
- [42] C. Ko, M. V. Pak, C. Swalina, and S. Hammes-Schiffer, Alternative wavefunction ansatz for including explicit electron-proton correlation in the nuclear-electronic orbital approach, *J. Chem. Phys.* **135**, 054106 (2011).
- [43] M. Hoshino, H. Nishizawa, and H. Nakai, Rigorous non-Born–Oppenheimer theory: Combination of explicitly correlated Gaussian method and nuclear orbital plus molecular orbital theory, *J. Chem. Phys.* **135**, 024111 (2011).
- [44] H. Nishizawa, Y. Imamura, Y. Ikabata, and H. Nakai, Development of the explicitly correlated Gaussian–nuclear orbital plus molecular orbital theory: Incorporation of electron–electron correlation, *Chem. Phys. Lett.* **533**, 100 (2012).
- [45] H. Nishizawa, M. Hoshino, Y. Imamura, and H. Nakai, Evaluation of electron repulsion integral of the explicitly correlated Gaussian–nuclear orbital plus molecular orbital theory, *Chem. Phys. Lett.* **521**, 142 (2012).
- [46] C. Swalina, M. V. Pak, and S. Hammes-Schiffer, Analysis of electron-positron wavefunctions in the nuclear-electronic orbital framework, *J. Chem. Phys.* **136**, 164105 (2012).
- [47] A. Sirjoosingh, M. V. Pak, C. Swalina, and S. Hammes-Schiffer, Reduced explicitly correlated Hartree-Fock approach within the nuclear-electronic orbital framework: Theoretical formulation, *J. Chem. Phys.* **139**, 034102 (2013).
- [48] A. Sirjoosingh, M. V. Pak, C. Swalina, and S. Hammes-Schiffer, Reduced explicitly correlated Hartree-Fock approach within the nuclear-electronic orbital framework: Applications to positronic molecular systems, *J. Chem. Phys.* **139**, 034103 (2013).
- [49] M. Díaz-Tinoco, J. Romero, J. V. Ortiz, A. Reyes, and R. Flores-Moreno, A generalized any-particle propagator theory: Prediction of proton affinities and acidity properties with the proton propagator, *J. Chem. Phys.* **138**, 194108 (2013).
- [50] Y. Suzuki, A. Abedi, N. T. Maitra, K. Yamashita, and E. K. U. Gross, Electronic Schrödinger equation with nonclassical nuclei, *Phys. Rev. A* **89**, 040501(R) (2014).
- [51] A. Sirjoosingh, M. V. Pak, K. R. Brorsen, and S. Hammes-Schiffer, Quantum treatment of protons with the reduced

- explicitly correlated Hartree-Fock approach, *J. Chem. Phys.* **142**, 214107 (2015).
- [52] K. R. Brorsen, A. Sirjoosingh, M. V. Pak, and S. Hammes-Schiffer, Nuclear-electronic orbital reduced explicitly correlated Hartree-Fock approach: Restricted basis sets and open-shell systems, *J. Chem. Phys.* **142**, 214108 (2015).
- [53] B. H. Ellis, S. Aggarwal, and A. Chakraborty, Development of the multicomponent coupled-cluster theory for investigation of multiexcitonic interactions, *J. Chem. Theory Comput.* **12**, 188 (2016).
- [54] Y. Tsukamoto, Y. Ikabata, J. Romero, A. Reyes, and H. Nakai, The divide-and-conquer second-order proton propagator method based on nuclear orbital plus molecular orbital theory for the efficient computation of proton binding energies, *Phys. Chem. Chem. Phys.* **18**, 27422 (2016).
- [55] B. H. Ellis and A. Chakraborty, Investigation of many-body correlation in biexcitonic systems using electron-hole multicomponent coupled-cluster theory, *J. Phys. Chem. C* **121**, 1291 (2017).
- [56] F. Pavošević and S. Hammes-Schiffer, Multicomponent coupled cluster singles and doubles and Brueckner doubles methods: Proton densities and energies, *J. Chem. Phys.* **151**, 074104 (2019).
- [57] F. Pavošević, T. Culpitt, and S. Hammes-Schiffer, Multicomponent coupled cluster singles and doubles theory within the nuclear-electronic orbital framework, *J. Chem. Theory Comput.* **15**, 338 (2019).
- [58] F. Pavošević and S. Hammes-Schiffer, Multicomponent equation-of-motion coupled cluster singles and doubles: Theory and calculation of excitation energies for positronium hydride, *J. Chem. Phys.* **150**, 161102 (2019).
- [59] F. Pavošević, B. J. G. Rousseau, and S. Hammes-Schiffer, Multicomponent orbital-optimized perturbation theory methods: Approaching coupled cluster accuracy at lower cost, *J. Phys. Chem. Lett.* **11**, 1578 (2020).
- [60] O. J. Fajen and K. R. Brorsen, Separation of electron-electron and electron-proton correlation in multicomponent orbital-optimized perturbation theory, *J. Chem. Phys.* **152**, 194107 (2020).
- [61] A. Muolo, A. Baiardi, R. Feldmann, and M. Reiher, Nuclear-electronic all-particle density matrix renormalization group, *J. Chem. Phys.* **152**, 204103 (2020).
- [62] V. J. Härkönen, R. van Leeuwen, and E. K. U. Gross, Many-body Green's function theory of electrons and nuclei beyond the Born-Oppenheimer approximation, *Phys. Rev. B* **101**, 235153 (2020).
- [63] K. R. Brorsen, Quantifying multireference character in multicomponent systems with heat-bath configuration interaction, *J. Chem. Theory Comput.* **16**, 2379 (2020).
- [64] F. Agostini and E. K. U. Gross, Exact factorization of the electron-nuclear wave function: Theory and applications, in *Quantum Chemistry and Dynamics of Excited States* (John Wiley & Sons, Ltd, 2020), Chap. 17, pp. 531–562.
- [65] O. J. Fajen and K. R. Brorsen, Multicomponent CASSCF revisited: Large active spaces are needed for qualitatively accurate protonic densities, *J. Chem. Theory Comput.* **17**, 965 (2021).
- [66] Z. Chen and J. Yang, Nucleus-electron correlation revising molecular bonding fingerprints from the exact wavefunction factorization, *J. Chem. Phys.* **155**, 104111 (2021).
- [67] E. Engel and R. M. Dreizler, *Density Functional Theory: An Advanced Course*, 1st ed. (Springer, Heidelberg, New York, 2011).
- [68] L. M. Sander, H. B. Shore, and L. J. Sham, Surface structure of electron-hole droplets, *Phys. Rev. Lett.* **31**, 533 (1973).
- [69] L. M. Sander, H. B. Shore, and L. J. Sham, Surface structure of electron-hole droplets, *Phys. Rev. Lett.* **31**, 1230 (1973).
- [70] R. K. Kalia and P. Vashishta, Surface structure of electron-hole drops in germanium and silicon, *Phys. Rev. B* **17**, 2655 (1978).
- [71] E. S. Kryachko, E. V. Ludeña, and V. Mujica, Formulation of N- and v-representable density functional theory. IV. Non-Born-Oppenheimer approach, *Int. J. Quantum Chem.* **40**, 589 (1991).
- [72] J. F. Capitani, R. F. Nalewajski, and R. G. Parr, Non-Born-Oppenheimer density functional theory of molecular systems, *J. Chem. Phys.* **76**, 568 (1982).
- [73] R. F. Nalewajski and J. F. Capitani, Density functional theory: Non-Born-Oppenheimer Legendre transforms and Maxwell relations, equilibrium and stability conditions, *J. Chem. Phys.* **77**, 2514 (1982).
- [74] R. F. Nalewajski, Internal density functional theory of molecular systems, *J. Chem. Phys.* **81**, 2088 (1984).
- [75] R. M. Nieminen, E. Boronski, and L. J. Lantto, Two-component density-functional theory: Application to positron states, *Phys. Rev. B* **32**, 1377 (1985).
- [76] E. Boroński and R. M. Nieminen, Electron-positron density-functional theory, *Phys. Rev. B* **34**, 3820 (1986).
- [77] T.-C. Li and P.-q. Tong, Time-dependent density-functional theory for multicomponent systems, *Phys. Rev. A* **34**, 529 (1986).
- [78] N. Gidopoulos, Kohn-Sham equations for multicomponent systems: The exchange and correlation energy functional, *Phys. Rev. B* **57**, 2146 (1998).
- [79] N. Barnea, Density functional theory for self-bound systems, *Phys. Rev. C* **76**, 067302 (2007).
- [80] J. Engel, Intrinsic-density functionals, *Phys. Rev. C* **75**, 014306 (2007).
- [81] A. Chakraborty, M. V. Pak, and S. Hammes-Schiffer, Properties of the exact universal functional in multicomponent density functional theory, *J. Chem. Phys.* **131**, 124115 (2009).
- [82] J. Messud, M. Bender, and E. Suraud, Density functional theory and Kohn-Sham scheme for self-bound systems, *Phys. Rev. C* **80**, 054314 (2009).
- [83] J. Messud, Generalization of internal density-functional theory and Kohn-Sham scheme to multicomponent self-bound systems, and link with traditional density-functional theory, *Phys. Rev. A* **84**, 052113 (2011).
- [84] N. I. Gidopoulos and E. K. U. Gross, Electronic non-adiabatic states: Towards a density functional theory beyond the Born-Oppenheimer approximation, *Phil. Trans. R. Soc. A* **372**, 20130059 (2014).
- [85] T. Culpitt, K. R. Brorsen, M. V. Pak, and S. Hammes-Schiffer, Multicomponent density functional theory embedding formulation, *J. Chem. Phys.* **145**, 044106 (2016).
- [86] R. Requist and E. K. U. Gross, Exact factorization-based density functional theory of electrons and nuclei, *Phys. Rev. Lett.* **117**, 193001 (2016).

- [87] Y. Suzuki, S. Hagiwara, and K. Watanabe, Time-dependent multicomponent density functional theory for coupled electron-positron dynamics, *Phys. Rev. Lett.* **121**, 133001 (2018).
- [88] R. Requist, C. R. Proetto, and E. K. U. Gross, Exact factorization-based density functional theory of electron-phonon systems, *Phys. Rev. B* **99**, 165136 (2019).
- [89] X. Xu and Y. Yang, Full-quantum descriptions of molecular systems from constrained nuclear–electronic orbital density functional theory, *J. Chem. Phys.* **153**, 074106 (2020).
- [90] M. J. Puska, A. P. Seitsonen, and R. M. Nieminen, Electron-positron Car-Parrinello methods: Self-consistent treatment of charge densities and ionic relaxations, *Phys. Rev. B* **52**, 10947 (1995).
- [91] T. Kreibich and E. K. U. Gross, Multicomponent density-functional theory for electrons and nuclei, *Phys. Rev. Lett.* **86**, 2984 (2001).
- [92] T. Ito, T. Yoshimoto, Y. Ohta, H. Kawabe, H. Nagao, and K. Nishikawa, Formulation and numerical approach to molecular systems by the Green function method without Born–Oppenheimer approximation II: Nucleus–electron correlation, *Int. J. Quantum Chem.* **100**, 918 (2004).
- [93] T. Udagawa and M. Tachikawa, H/D isotope effect on porphine and porphycene molecules with multicomponent hybrid density functional theory, *J. Chem. Phys.* **125**, 244105 (2006).
- [94] Y. Imamura, H. Kiryu, and H. Nakai, Colle-Salvetti-type correction for electron–nucleus correlation in the nuclear orbital plus molecular orbital theory, *J. Comput. Chem.* **29**, 735 (2008).
- [95] A. Chakraborty, M. V. Pak, and S. Hammes-Schiffer, Development of electron-proton density functionals for multicomponent density functional theory, *Phys. Rev. Lett.* **101**, 153001 (2008).
- [96] T. Kreibich, R. van Leeuwen, and E. K. U. Gross, Multicomponent density-functional theory for electrons and nuclei, *Phys. Rev. A* **78**, 022501 (2008).
- [97] Y. Imamura, Y. Tsukamoto, H. Kiryu, and H. Nakai, Extension of density functional theory to nuclear orbital plus molecular orbital theory: Self-consistent field calculations with the colle-salvetti electron–nucleus correlation functional, *Bull. Chem. Soc. Jpn.* **82**, 1133 (2009).
- [98] A. Sirjoosingh, M. V. Pak, and S. Hammes-Schiffer, Derivation of an electron–proton correlation functional for multicomponent density functional theory within the nuclear–electronic orbital approach, *J. Chem. Theory Comput.* **7**, 2689 (2011).
- [99] A. Sirjoosingh, M. V. Pak, and S. Hammes-Schiffer, Multicomponent density functional theory study of the interplay between electron–electron and electron–proton correlation, *J. Chem. Phys.* **136**, 174114 (2012).
- [100] J. Kuriplach and B. Barbiellini, Improved generalized gradient approximation for positron states in solids, *Phys. Rev. B* **89**, 155111 (2014).
- [101] T. Udagawa, T. Tsuneda, and M. Tachikawa, Electron-nucleus correlation functional for multicomponent density-functional theory, *Phys. Rev. A* **89**, 052519 (2014).
- [102] A. Zubiaga, F. Tuomisto, and M. J. Puska, Full-correlation single-particle positron potentials for a positron and positronium interacting with atoms, *Phys. Rev. A* **89**, 052707 (2014).
- [103] J. Wiktor, G. Jomard, and M. Torrent, Two-component density functional theory within the projector augmented-wave approach: Accurate and self-consistent computations of positron lifetimes and momentum distributions, *Phys. Rev. B* **92**, 125113 (2015).
- [104] Y. Yang, K. R. Brorsen, T. Culpitt, M. V. Pak, and S. Hammes-Schiffer, Development of a practical multicomponent density functional for electron-proton correlation to produce accurate proton densities, *J. Chem. Phys.* **147**, 114113 (2017).
- [105] K. R. Brorsen, P. E. Schneider, and S. Hammes-Schiffer, Alternative forms and transferability of electron-proton correlation functionals in nuclear-electronic orbital density functional theory, *J. Chem. Phys.* **149**, 044110 (2018).
- [106] G. Kolesov, E. Kaxiras, and E. Manousakis, Density functional theory beyond the Born-Oppenheimer approximation: Accurate treatment of the ionic zero-point motion, *Phys. Rev. B* **98**, 195112 (2018).
- [107] Z. Tao, Y. Yang, and S. Hammes-Schiffer, Multicomponent density functional theory: Including the density gradient in the electron-proton correlation functional for hydrogen and deuterium, *J. Chem. Phys.* **151**, 124102 (2019).
- [108] M. Goli and S. Shahbazian, Two-component density functional theory for muonic molecules: Inclusion of the electron–positive muon correlation functional, *J. Chem. Phys.* **156**, 044104 (2022).
- [109] J. M. McMahon, M. A. Morales, C. Pierleoni, and D. M. Ceperley, The properties of hydrogen and helium under extreme conditions, *Rev. Mod. Phys.* **84**, 1607 (2012).
- [110] W. J. Nellis, Wigner and Huntington: The long quest for metallic hydrogen, *High Press. Res.* **33**, 369 (2013).
- [111] E. Gregoryanz, C. Ji, P. Dalladay-Simpson, B. Li, R. T. Howie, and H.-K. Mao, Everything you always wanted to know about metallic hydrogen but were afraid to ask, *Matter Radiat. Extrem.* **5**, 038101 (2020).
- [112] I. F. Silvera and R. Dias, Phases of the hydrogen isotopes under pressure: Metallic hydrogen, *Adv. Phys.-X* **6**, 1961607 (2021).
- [113] H. Xu and J.-P. Hansen, Density-functional theory of pair correlations in metallic hydrogen, *Phys. Rev. E* **57**, 211 (1998).
- [114] H. Kitamura, S. Tsuneyuki, T. Ogitsu, and T. Miyake, Quantum distribution of protons in solid molecular hydrogen at megabar pressures, *Nature* **404**, 259 (2000).
- [115] H. Xu, Density functional theory applied to metallic hydrogen: Pair correlations and phase transitions, *J. Phys.: Condens. Matter* **14**, 9109 (2002).
- [116] A. F. Goncharov and J. Crowhurst, Proton delocalization under extreme conditions of high pressure and temperature, *Phase Transit.* **80**, 1051 (2007).
- [117] C. Pierleoni, K. T. Delaney, M. A. Morales, D. M. Ceperley, and M. Holzmann, Trial wave functions for high-pressure metallic hydrogen, *Comput. Phys. Commun.* **179**, 89 (2008).
- [118] J. M. McMahon and D. M. Ceperley, Ground-state structures of atomic metallic hydrogen, *Phys. Rev. Lett.* **106**, 165302 (2011).
- [119] J. McMinis, R. C. Clay, D. Lee, and M. A. Morales, Molecular to atomic phase transition in hydrogen under high pressure, *Phys. Rev. Lett.* **114**, 105305 (2015).
- [120] K. Liao, X.-Z. Li, A. Alavi, and A. Grüneis, A comparative study using state-of-the-art electronic structure theories on solid hydrogen phases under high pressures, *npj Comput Mater* **5**, 1 (2019).

- [121] C. M. Tenney, K. L. Sharkey, and J. M. McMahon, Possibility of metastable atomic metallic hydrogen, *Phys. Rev. B* **102**, 224108 (2020).
- [122] V. Gorelov, M. Holzmann, D. M. Ceperley, and C. Pierleoni, Energy gap closure of crystalline molecular hydrogen with pressure, *Phys. Rev. Lett.* **124**, 116401 (2020).
- [123] L. Monacelli, I. Errea, M. Calandra, and F. Mauri, Black metal hydrogen above 360 GPa driven by proton quantum fluctuations, *Nat. Phys.* **17**, 63 (2021).
- [124] H. Niu, Y. Yang, S. Jensen, M. Holzmann, C. Pierleoni, and D. M. Ceperley, Stable solid molecular hydrogen above 900 K from a machine-learned potential trained with diffusion quantum Monte Carlo, *Phys. Rev. Lett.* **130**, 076102 (2023).
- [125] K. R. Allen and T. Dunn, Variational method for the ground state of multispecies quantum fluids, *Phys. Rev.* **170**, 293 (1968).
- [126] A. A. Broyles, A. A. Barker, T. Dunn, and M. A. Pokrant, Methods for computing distribution functions for electrons and nuclei in fluids, *Int. J. Quantum Chem.* **3**, 293 (1969).
- [127] A. A. Barker, Effective Potentials between the Components of a Hydrogenous Plasma, *J. Chem. Phys.* **55**, 1751 (1971).
- [128] M. A. Pokrant, A. A. Broyles, and R. L. Coldwell, Nonzero temperature variational principle, *Int. J. Quantum Chem.* **8**, 403 (1974).
- [129] T. Chakraborty and P. Pietiläinen, Variational approach to the ground state of the electron-hole liquid, *Phys. Rev. Lett.* **49**, 1034 (1982).
- [130] M. W. C. Dharma-wardana and F. Perrot, Density-functional theory of hydrogen plasmas, *Phys. Rev. A* **26**, 2096 (1982).
- [131] P. Pietiläinen, L. Lantto, and A. Kallio, Variational approach to two-component coulomb liquids, in *Recent Progress in Many-Body Theories*, Lecture Notes in Physics, edited by H. Kümmel and M. L. Ristig (Springer, Berlin, Heidelberg, 1984), pp. 181–188.
- [132] R. F. Bishop and W. A. Lahoz, Two-component Fermi systems. I. Fluid coupled cluster theory, *J. Phys. A: Math. Gen.* **20**, 4203 (1987).
- [133] W. A. Lahoz and R. F. Bishop, Two-component Fermi systems: II. Superfluid coupled cluster theory, *Z. Physik B - Condensed Matter* **73**, 363 (1988).
- [134] F. Perrot and M. W. C. Dharma-wardana, Equation of state and transport properties of an interacting multispecies plasma: Application to a multiply ionized Al plasma, *Phys. Rev. E* **52**, 5352 (1995).
- [135] B. Hetényi, Approximate solution of variational wave functions for strongly correlated systems: Description of bound excitons in metals and insulators, *Phys. Rev. B* **82**, 115104 (2010).
- [136] M. W. C. Dharma-wardana, Electron-ion and ion-ion potentials for modeling warm dense matter: Applications to laser-heated or shock-compressed Al and Si, *Phys. Rev. E* **86**, 036407 (2012).
- [137] R. G. Parr and W. Yang, *Density-Functional Theory of Atoms and Molecules* (Oxford University Press, New York, 1994).
- [138] G. D. Mahan, *Many-Particle Physics*, 3rd ed. (Springer, New York, 2000).
- [139] W. F. Brinkman and T. M. Rice, Electron-hole liquids in semiconductors, *Phys. Rev. B* **7**, 1508 (1973).
- [140] J. Arponen and E. Pajanne, Electron liquid in collective description. III. Positron annihilation, *Ann. Phys.* **121**, 343 (1979).
- [141] P. Pietiläinen and A. Kallio, Hypernetted-chain theory of charged impurity with mixture formalism, *Phys. Rev. B* **27**, 224 (1983).
- [142] L. V. Keldysh, The electron-hole liquid in semiconductors, *Contemp. Phys.* **27**, 395 (1986).
- [143] L. J. Lantto, Variational theory of multicomponent quantum fluids: An application to positron-electron plasmas at $T = 0$, *Phys. Rev. B* **36**, 5160 (1987).
- [144] N. D. Drummond, P. López Ríos, R. J. Needs, and C. J. Pickard, Quantum Monte Carlo study of a positron in an electron gas, *Phys. Rev. Lett.* **107**, 207402 (2011).
- [145] M. Manninen, R. Nieminen, P. Hautojärvi, and J. Arponen, Electrons and positrons in metal vacancies, *Phys. Rev. B* **12**, 4012 (1975).
- [146] R. P. Gupta and R. W. Siegel, Electron and positron densities and the temperature dependence of the positron lifetime in a vacancy in aluminum, *Phys. Rev. Lett.* **39**, 1212 (1977).
- [147] M. J. Puska and R. M. Nieminen, Defect spectroscopy with positrons: A general calculational method, *J. Phys. F: Met. Phys.* **13**, 333 (1983).
- [148] C. O. Almbladh, U. von Barth, Z. D. Popovic, and M. J. Stott, Screening of a proton in an electron gas, *Phys. Rev. B* **14**, 2250 (1976).
- [149] A. Kallio, P. Pietiläinen, and L. Lantto, Hypernetted chain theory of charged impurity, *Phys. Scr.* **25**, 943 (1982).
- [150] J. Gondzik and H. Stachowiak, Screening of positive particles in jellium, *J. Phys. C: Solid State Phys.* **18**, 5399 (1985).
- [151] H. Stachowiak, Screening of a proton moving through the electron gas, *Phys. Stat. Sol. (B)* **121**, 307 (1984).
- [152] H. Stachowiak, Screening of a proton moving through the electron gas. II. Kinetic Properties of the screening cloud, *Phys. Stat. Sol. (B)* **140**, 521 (1987).
- [153] H. Stachowiak, Screening of a proton moving through the electron gas III. Computation of the momentum distribution of the screening cloud, *Phys. Stat. Sol. (B)* **141**, 447 (1987).
- [154] L. Deng, Y. Yuan, F. L. Pratt, W. Zhang, Z. Pan, and B. Ye, Two-component density functional theory study of quantized muons in solids, *Phys. Rev. B* **107**, 094433 (2023).
- [155] R. Colle and O. Salvetti, Approximate calculation of the correlation energy for the closed shells, *Theoret. Chim. Acta* **37**, 329 (1975).
- [156] N. C. Handy, The importance of Colle–Salvetti for computational density functional theory, *Theor. Chem. Acc.* **123**, 165 (2009).
- [157] K. R. Brorsen, Y. Yang, and S. Hammes-Schiffer, Multicomponent density functional theory: Impact of nuclear quantum effects on proton affinities and geometries, *J. Phys. Chem. Lett.* **8**, 3488 (2017).
- [158] Y. Yang, T. Culpitt, and S. Hammes-Schiffer, Multicomponent time-dependent density functional theory: Proton and electron excitation energies, *J. Phys. Chem. Lett.* **9**, 1765 (2018).
- [159] Z. Tao, Q. Yu, S. Roy, and S. Hammes-Schiffer, Direct dynamics with nuclear–electronic orbital density functional theory, *Acc. Chem. Res.* **54**, 4131 (2021).
- [160] J. Kohanoff, *Electronic Structure Calculations for Solids and Molecules: Theory and Computational Methods*, 1st ed. (Cambridge University Press, Cambridge, UK, New York, 2006).

- [161] A. D. Bochevarov, E. F. Valeev, and C. David Sherrill, The electron and nuclear orbitals model: Current challenges and future prospects, *Mol. Phys.* **102**, 111 (2004).
- [162] M. Moshinsky and Y. F. Smirnov, *Harmonic Oscillator in Modern Physics* (Harwood Academic Publishers, Amsterdam, 1996).
- [163] B. Sutherland, *Beautiful Models: 70 Years of Exactly Solved Quantum Many-Body Problems*, 1st ed. (World Scientific, Singapore, 2004).
- [164] J. A. Maruhn, P.-G. Reinhard, and E. Suraud, *Simple Models of Many-Fermion Systems*, 1st ed. (Springer, Berlin, Heidelberg, 2014).
- [165] N. H. March and G. G. N. Angilella, *Exactly Solvable Models in Many-Body Theory* (World Scientific, Singapore, 2016).
- [166] L. Piela, *Ideas of Quantum Chemistry*, 1st ed. (Elsevier Science, Amsterdam; Boston, 2007).
- [167] N. R. Kestner and O. Sinanoğlu, Study of electron correlation in helium-like systems using an exactly soluble model, *Phys. Rev.* **128**, 2687 (1962).
- [168] E. Santos, Calculo aproximado de la energia de correlacion entre dos electrones, *Anal. R. Soc. Esp. Fis. Quim.* **64**, 177 (1968).
- [169] D. F.-t. Tuan, Double perturbation theory for He-like systems, *J. Chem. Phys.* **50**, 2740 (1969).
- [170] R. J. White and W. B. Brown, Perturbation theory of the Hooke's law model for the two-electron atom, *J. Chem. Phys.* **53**, 3869 (1970).
- [171] J. M. Benson and W. B. Brown, Perturbation energies for the Hooke's law model of the two-electron atom, *J. Chem. Phys.* **53**, 3880 (1970).
- [172] S. Kais, D. R. Herschbach, and R. D. Levine, Dimensional scaling as a symmetry operation, *J. Chem. Phys.* **91**, 7791 (1989).
- [173] A. Samanta and S. K. Ghosh, Correlation in an exactly solvable two-particle quantum system, *Phys. Rev. A* **42**, 1178 (1990).
- [174] S. K. Ghosh and A. Samanta, Study of correlation effects in an exactly solvable model two-electron system, *J. Chem. Phys.* **94**, 517 (1991).
- [175] M. Taut, Two electrons in an external oscillator potential: Particular analytic solutions of a Coulomb correlation problem, *Phys. Rev. A* **48**, 3561 (1993).
- [176] A. Turbiner, Two electrons in an external oscillator potential: The hidden algebraic structure, *Phys. Rev. A* **50**, 5335 (1994).
- [177] H. F. King, The electron correlation cusp, *Theoret. Chim. Acta* **94**, 345 (1996).
- [178] J.-L. Zhu, Z.-Q. Li, J.-Z. Yu, K. Ohno, and Y. Kawazoe, Size and shape effects of quantum dots on two-electron spectra, *Phys. Rev. B* **55**, 15819 (1997).
- [179] G. Lamouche and G. Fishman, Two interacting electrons in a three-dimensional parabolic quantum dot: A simple solution, *J. Phys.: Condens. Matter* **10**, 7857 (1998).
- [180] J. Cioslowski and K. Pernal, The ground state of harmonium, *J. Chem. Phys.* **113**, 8434 (2000).
- [181] T. M. Henderson, K. Runge, and R. J. Bartlett, Electron correlation in artificial atoms, *Chem. Phys. Lett.* **337**, 138 (2001).
- [182] E. Romera, Electron-pair uncertainty relationships and the intracule-extracule isomorphism, *J. Phys. B: At. Mol. Opt. Phys.* **35**, L309 (2002).
- [183] L. Cyrnek, The energy spectrum of harmonium, in *Symmetry and Structural Properties of Condensed Matter* (World Scientific, Singapore, 2003), pp. 373–377.
- [184] D. P. O'Neill and P. M. W. Gill, Wave functions and two-electron probability distributions of the Hooke's-law atom and helium, *Phys. Rev. A* **68**, 022505 (2003).
- [185] S. Mandal, P. K. Mukherjee, and G. H. F. Diercksen, Two electrons in a harmonic potential: An approximate analytical solution, *J. Phys. B: At. Mol. Opt. Phys.* **36**, 4483 (2003).
- [186] C. Amovilli, Á. Nagy, and N. H. March, Approximate ansatz for the expansion of the spherically averaged wave function in terms of interelectronic separation r_{12} for the Hookean atom, atomic ions, and the H_2 molecule, *Int. J. Quantum Chem.* **95**, 21 (2003).
- [187] J. Karwowski and L. Cyrnek, Harmonium, *Ann. Phys.* **516**, 181 (2004).
- [188] P. M. W. Gill and D. P. O'Neill, Electron correlation in Hooke's law atom in the high-density limit, *J. Chem. Phys.* **122**, 094110 (2005).
- [189] J. Katriel, S. Roy, and M. Springborg, Effect of the one-body potential on interelectronic correlation in two-electron systems, *J. Chem. Phys.* **123**, 104104 (2005).
- [190] A. Akbari, N. H. March, and A. Rubio, Momentum density and spatial form of correlated density matrix in model two-electron atoms with harmonic confinement, *Phys. Rev. A* **76**, 032510 (2007).
- [191] S. Ragot, Comments on the Hartree-Fock description of Hooke's atom and suggestion for an accurate closed-form orbital, *J. Chem. Phys.* **128**, 164104 (2008).
- [192] P.-F. Loos and P. M. W. Gill, Correlation energy of two electrons in the high-density limit, *J. Chem. Phys.* **131**, 241101 (2009).
- [193] E. Matito, J. Cioslowski, and S. F. Vyboishchikov, Properties of harmonium atoms from FCI calculations: Calibration and benchmarks for the ground state of the two-electron species, *Phys. Chem. Chem. Phys.* **12**, 6712 (2010).
- [194] K. Ebrahimi-Fard and J. M. Gracia-Bondía, Harmonium as a laboratory for mathematical chemistry, *J. Math. Chem.* **50**, 440 (2012).
- [195] J. Karwowski and H. A. Witek, Biconfluent Heun equation in quantum chemistry: Harmonium and related systems, *Theor. Chem. Acc.* **133**, 1494 (2014).
- [196] I. Nagy and M. L. Glasser, Information-theoretic aspects of friction in the quantum mechanics of an interacting two-electron harmonic atom, *J. Math. Chem.* **53**, 1274 (2015).
- [197] J. Cioslowski and K. Strasburger, Harmonium atoms at weak confinements: The formation of the Wigner molecules, *J. Chem. Phys.* **146**, 044308 (2017).
- [198] A. Galiautdinov, Ground state of an exciton in a three-dimensional parabolic quantum dot: Convergent perturbative calculation, *Phys. Lett. A* **382**, 72 (2018).
- [199] J. Cioslowski, Natural orbitals of the ground state of the two-electron harmonium atom, *Theor. Chem. Acc.* **137**, 173 (2018).
- [200] T. M. Rusin and W. Zawadzki, Pauli exclusion operator: An example of Hooke's atom, *Phys. Rev. A* **103**, 052221 (2021).
- [201] A. G. Ushveridze, *Quasi-Exactly Solvable Models in Quantum Mechanics*, 1st ed. (Institute Of Physics Publishing, Bristol England; Philadelphia, 1994).
- [202] K. Burke, J. P. Perdew, and M. Levy, Semilocal density functionals for exchange and correlation: Theory and applications,

- in *Theoretical and Computational Chemistry*, Modern Density Functional Theory, Vol. 2, edited by J. M. Seminario and P. Politzer (Elsevier, Amsterdam, 1995), pp. 29–74.
- [203] P. M. Laufer and J. B. Krieger, Test of density-functional approximations in an exactly soluble model, *Phys. Rev. A* **33**, 1480 (1986).
- [204] R. W. Hall, Comparison of path integral and density functional techniques in a model two-electron system, *J. Phys. Chem.* **93**, 5628 (1989).
- [205] A. Samanta and S. K. Ghosh, Density-functional approach to the calculation of correlation energies of two-electron atoms and ions, *Phys. Rev. A* **43**, 6395 (1991).
- [206] A. Samanta and S. K. Ghosh, Study of correlation in Kohn–Sham density functional theory for exactly solvable two-electron systems, *Chem. Phys. Lett.* **180**, 121 (1991).
- [207] S. Kais, D. R. Herschbach, N. C. Handy, C. W. Murray, and G. J. Laming, Density functionals and dimensional renormalization for an exactly solvable model, *J. Chem. Phys.* **99**, 417 (1993).
- [208] C. Filippi, C. J. Umrigar, and M. Taut, Comparison of exact and approximate density functionals for an exactly soluble model, *J. Chem. Phys.* **100**, 1290 (1994).
- [209] C.-J. Huang and C. J. Umrigar, Local correlation energies of two-electron atoms and model systems, *Phys. Rev. A* **56**, 290 (1997).
- [210] M. Taut, A. Ernst, and H. Eschrig, Two electrons in an external oscillator potential: Exact solution versus one-particle approximations, *J. Phys. B: At. Mol. Opt. Phys.* **31**, 2689 (1998).
- [211] Z. Qian and V. Sahni, Physics of transformation from Schrödinger theory to Kohn–Sham density-functional theory: Application to an exactly solvable model, *Phys. Rev. A* **57**, 2527 (1998).
- [212] N. H. March, T. Gál, and Á. Nagy, Differential equation for the ground-state electron density in a Hookean atom with two electrons repelling coulombically, *Chem. Phys. Lett.* **292**, 384 (1998).
- [213] K.-C. Lam, F. G. Cruz, and K. Burke, Virial exchange–correlation energy density in Hooke’s atom, *Int. J. Quantum Chem.* **69**, 533 (1998).
- [214] P. Hessler, J. Park, and K. Burke, Several theorems in time-dependent density functional theory, *Phys. Rev. Lett.* **82**, 378 (1999).
- [215] P. Hessler, J. Park, and K. Burke, Erratum: Several theorems in time-dependent density functional theory [Phys. Rev. Lett. 82, 378 (1999)], *Phys. Rev. Lett.* **83**, 5184(E) (1999).
- [216] S. Ivanov, K. Burke, and M. Levy, Exact high-density limit of correlation potential for two-electron density, *J. Chem. Phys.* **110**, 10262 (1999).
- [217] N. H. March, C. Amovilli, and D. J. Klein, The wavefunction when antiparallel spin electrons coincide and its relation to the ground-state electron density in the Hookean atom, *Chem. Phys. Lett.* **325**, 645 (2000).
- [218] D. Frydel, W. M. Terilla, and K. Burke, Adiabatic connection from accurate wave-function calculations, *J. Chem. Phys.* **112**, 5292 (2000).
- [219] E. V. Ludeña, V. Karasiev, A. Artemiev, and D. Gómez, Functional N-representability in Density Matrix and Density Functional Theory: An Illustration for Hooke’s Atom, in *Many-Electron Densities and Reduced Density Matrices*, Mathematical and Computational Chemistry, edited by J. Cioslowski (Springer US, Boston, MA, 2000), pp. 209–230.
- [220] A. Artemiev, E. V. Ludeña, and V. Karasiev, A DFT variational approach to Hooke’s atom based on local-scaling transformations, *J. Mol. Struct.: THEOCHEM* **580**, 47 (2002).
- [221] C. Amovilli and N. H. March, Exact density matrix for a two-electron model atom and approximate proposals for realistic two-electron systems, *Phys. Rev. A* **67**, 022509 (2003).
- [222] A. Holas, I. A. Howard, and N. H. March, Wave functions and low-order density matrices for a class of two-electron ‘artificial atoms’ embracing Hookean and Moshinsky models, *Phys. Lett. A* **310**, 451 (2003).
- [223] N. March and A. Holas, Kinetic energy density of the two-electron Hookean atom in terms of the ground-state electron density, *J. Math. Chem.* **33**, 163 (2003).
- [224] N. H. March and E. V. Ludeña, Effective one-body potential of DFT plus correlated kinetic energy density for two-electron spherical model atoms, *Phys. Lett. A* **330**, 16 (2004).
- [225] E. V. Ludeña, D. Gómez, V. Karasiev, and P. Nieto, Exact analytic total energy functional for Hooke’s atom generated by local-scaling transformations, *Int. J. Quantum Chem.* **99**, 297 (2004).
- [226] J. Katriel, S. Roy, and M. Springborg, A study of the adiabatic connection for two-electron systems, *J. Chem. Phys.* **121**, 12179 (2004).
- [227] P. Capuzzi, N. H. March, and M. P. Tosi, Differential equation for the ground-state density of artificial two-electron atoms with harmonic confinement, *J. Phys. A: Math. Gen.* **38**, L439 (2005).
- [228] S. Ragot, Exact Kohn–Sham versus Hartree–Fock in momentum space: Examples of two-fermion systems, *J. Chem. Phys.* **125**, 014106 (2006).
- [229] D. Gómez, E. V. Ludeña, V. Karasiev, and P. Nieto, Application of exact analytic total energy functional for Hooke’s atom to He, Li⁺ and Be⁺⁺: An examination of the universality of the energy functional in DFT, *Theor. Chem. Acc.* **116**, 608 (2006).
- [230] W. Zhu and S. B. Trickey, Exact density functionals for two-electron systems in an external magnetic field, *J. Chem. Phys.* **125**, 094317 (2006).
- [231] M. Seidl, P. Gori-Giorgi, and A. Savin, Strictly correlated electrons in density-functional theory: A general formulation with applications to spherical densities, *Phys. Rev. A* **75**, 042511 (2007).
- [232] J. Katriel, M. Bauer, M. Springborg, S. P. McCarthy, and A. J. Thakkar, Nonlocal Wigner-like correlation energy density functional: Parametrization and tests on two-electron systems, *J. Chem. Phys.* **127**, 024101 (2007).
- [233] J. P. Coe, A. Sudbery, and I. D’Amico, Entanglement and density-functional theory: Testing approximations on Hooke’s atom, *Phys. Rev. B* **77**, 205122 (2008).
- [234] J. P. Coe, A. Sudbery, and I. D’Amico, Erratum: Entanglement and density-functional theory: Testing approximations on Hooke’s atom [Phys. Rev. B 77, 205122 (2008)], *Phys. Rev. B* **82**, 089902(E) (2010).
- [235] J. Sun, Extension to negative values of the coupling constant of adiabatic connection for interaction-strength interpolation, *J. Chem. Theory Comput.* **5**, 708 (2009).
- [236] P. Gori-Giorgi and A. Savin, Study of the discontinuity of the exchange-correlation potential in an exactly soluble case, *Int. J. Quantum Chem.* **109**, 2410 (2009).

- [237] M. Seidl and P. Gori-Giorgi, Adiabatic connection at negative coupling strengths, *Phys. Rev. A* **81**, 012508 (2010).
- [238] J. Cioslowski, M. Piris, and E. Matito, Robust validation of approximate 1-matrix functionals with few-electron harmonium atoms, *J. Chem. Phys.* **143**, 214101 (2015).
- [239] R. S. Chauhan and M. K. Harbola, Study of adiabatic connection in density functional theory with an accurate wavefunction for two-electron spherical systems, *Int. J. Quantum Chem.* **117**, e25344 (2017).
- [240] D. P. Kooi and P. Gori-Giorgi, Local and global interpolations along the adiabatic connection of DFT: A study at different correlation regimes, *Theor. Chem. Acc.* **137**, 166 (2018).
- [241] R. Singh, A. Kumar, M. K. Harbola, and P. Samal, Semianalytical wavefunctions and Kohn–Sham exchange–correlation potentials for two-electron atomic systems in two-dimensions, *J. Phys. B: At. Mol. Opt. Phys.* **53**, 035001 (2020).
- [242] M. Goli and S. Shahbazian, Deciphering the “chemical” nature of the exotic isotopes of hydrogen by the MC-QTAIM analysis: The positively charged muon and the muonic helium as new members of the periodic table, *Phys. Chem. Chem. Phys.* **16**, 6602 (2014).
- [243] M. Goli and S. Shahbazian, Topological and AIM analyses beyond the Born–Oppenheimer paradigm: New opportunities, *Comput. Theor. Chem.* **1053**, 96 (2015).
- [244] M. Goli and S. Shahbazian, Where to place the positive muon in the Periodic Table? *Phys. Chem. Chem. Phys.* **17**, 7023 (2015).
- [245] M. Goli and S. Shahbazian, Developing effective electronic-only coupled-cluster and Møller–Plesset perturbation theories for the muonic molecules, *Phys. Chem. Chem. Phys.* **20**, 16749 (2018).
- [246] J. Stetzler and V. A. Rassolov, Comparison of Born–Oppenheimer approximation and electron–nuclear correlation, *Mol. Phys.* **121**, e2106321 (2023).
- [247] F. M. Fernández, The confined hydrogen atom with a moving nucleus, *Eur. J. Phys.* **31**, 285 (2010).
- [248] F. M. Fernández, Variational treatment of the confined hydrogen atom with a moving nucleus, *Eur. J. Phys.* **31**, 611 (2010).
- [249] F. M. Fernández, N. Aquino, and A. Flores-Riveros, Variational approach to the confined hydrogen atom with a moving nucleus, *Int. J. Quantum Chem.* **112**, 823 (2012).
- [250] J. M. Randazzo and C. A. Rios, Endohedrally confined hydrogen atom with a moving nucleus, *J. Phys. B: At. Mol. Opt. Phys.* **49**, 235003 (2016).
- [251] Y. Kayanuma, Wannier exciton in microcrystals, *Solid State Commun.* **59**, 405 (1986).
- [252] S. V. Nair, S. Sinha, and K. C. Rustagi, Quantum size effects in spherical semiconductor microcrystals, *Phys. Rev. B* **35**, 4098 (1987).
- [253] Y. Kayanuma, Quantum-size effects of interacting electrons and holes in semiconductor microcrystals with spherical shape, *Phys. Rev. B* **38**, 9797 (1988).
- [254] Y. Kayanuma and H. Momiji, Incomplete confinement of electrons and holes in microcrystals, *Phys. Rev. B* **41**, 10261 (1990).
- [255] J. M. Elward, J. Hoffman, and A. Chakraborty, Investigation of electron–hole correlation using explicitly correlated configuration interaction method, *Chem. Phys. Lett.* **535**, 182 (2012).
- [256] J. M. Elward, B. Thallinger, and A. Chakraborty, Calculation of electron–hole recombination probability using explicitly correlated Hartree–Fock method, *J. Chem. Phys.* **136**, 124105 (2012).
- [257] D. McIntyre, C. Manogue, and J. Tate, *Quantum Mechanics: A Paradigms Approach*, 1st ed. (Pearson, Boston, 2012).
- [258] D. Lin-Vien, N. B. Colthup, W. G. Fateley, and J. G. Grasselli, *The Handbook of Infrared and Raman Characteristic Frequencies of Organic Molecules*, 1st ed. (Academic Press, Boston, 1991).
- [259] U. A. Jayasooriya, F. L. Pratt, G. M. Aston, S. Hall, P. L. Hubbard, and M. McCoustra, A strategy for the measurement of the vibrations of a muoniated radical centre: Experimental evidence, *ChemPhysChem* **5**, 257 (2004).
- [260] C. J. Umrigar and X. Gonze, Accurate exchange–correlation potentials and total-energy components for the helium isoelectronic series, *Phys. Rev. A* **50**, 3827 (1994).
- [261] O. V. Gritsenko, R. van Leeuwen, and E. J. Baerends, Molecular Kohn–Sham exchange–correlation potential from the correlated *ab initio* electron density, *Phys. Rev. A* **52**, 1870 (1995).
- [262] O. V. Gritsenko, R. van Leeuwen, and E. J. Baerends, Molecular exchange–correlation Kohn–Sham potential and energy density from *ab initio* first- and second-order density matrices: Examples for XH (X=Li, B, F), *J. Chem. Phys.* **104**, 8535 (1996).
- [263] A. A. Kananenka, S. V. Kohut, A. P. Gaiduk, I. G. Ryabinkin, and V. N. Staroverov, Efficient construction of exchange and correlation potentials by inverting the Kohn–Sham equations, *J. Chem. Phys.* **139**, 074112 (2013).
- [264] I. G. Ryabinkin, S. V. Kohut, and V. N. Staroverov, Reduction of electronic wave functions to Kohn–Sham effective potentials, *Phys. Rev. Lett.* **115**, 083001 (2015).
- [265] B. Kanungo, P. M. Zimmerman, and V. Gavini, Exact exchange–correlation potentials from ground-state electron densities, *Nat. Commun.* **10**, 4497 (2019).
- [266] A. Kumar, R. Singh, and M. K. Harbola, Accurate effective potential for density amplitude and the corresponding Kohn–Sham exchange–correlation potential calculated from approximate wavefunctions, *J. Phys. B: At. Mol. Opt. Phys.* **53**, 165002 (2020).
- [267] B. Kanungo, P. M. Zimmerman, and V. Gavini, A comparison of exact and model exchange–correlation potentials for molecules, *J. Phys. Chem. Lett.* **12**, 12012 (2021).
- [268] T. Udagawa, T. Tsuneda, and M. Tachikawa, Development of Colle–Salvetti type electron–nucleus correlation functional for MC_DFT, *AIP Conf. Proc.* **1702**, 090065 (2015).
- [269] M. V. Pak, A. Chakraborty, and S. Hammes-Schiffer, Density functional theory treatment of electron correlation in the nuclear–electronic orbital approach, *J. Phys. Chem. A* **111**, 4522 (2007).
- [270] M. W. Schmidt, K. K. Baldridge, J. A. Boatz, S. T. Elbert, M. S. Gordon, J. H. Jensen, S. Koseki, N. Matsunaga, K. A. Nguyen, S. Su, T. L. Windus, M. Dupuis, and J. A. Montgomery, General atomic and molecular electronic structure system, *J. Comput. Chem.* **14**, 1347 (1993).
- [271] Q. Zhao, R. C. Morrison, and R. G. Parr, From electron densities to Kohn–Sham kinetic energies, orbital energies, exchange–correlation potentials, and exchange–correlation energies, *Phys. Rev. A* **50**, 2138 (1994).

- [272] F. G. Cruz, K.-C. Lam, and K. Burke, Exchange-correlation energy density from virial theorem, *J. Phys. Chem. A* **102**, 4911 (1998).
- [273] K. Burke, F. G. Cruz, and K.-C. Lam, Unambiguous exchange-correlation energy density, *J. Chem. Phys.* **109**, 8161 (1998).
- [274] M.-C. Kim, E. Sim, and K. Burke, Understanding and reducing errors in density functional calculations, *Phys. Rev. Lett.* **111**, 073003 (2013).
- [275] E. Sim, S. Song, and K. Burke, Quantifying density errors in DFT, *J. Phys. Chem. Lett.* **9**, 6385 (2018).
- [276] S. Vuckovic, S. Song, J. Kozłowski, E. Sim, and K. Burke, Density functional analysis: The theory of density-corrected DFT, *J. Chem. Theory Comput.* **15**, 6636 (2019).
- [277] U. von Barth, Basic density-functional theory—an overview, *Phys. Scr.* **2004**, 9 (2004).
- [278] A. J. Cohen, P. Mori-Sánchez, and W. Yang, Insights into current limitations of density functional theory, *Science* **321**, 792 (2008).
- [279] A. J. Cohen, P. Mori-Sánchez, and W. Yang, Challenges for density functional theory, *Chem. Rev.* **112**, 289 (2012).
- [280] K. Burke, Perspective on density functional theory, *J. Chem. Phys.* **136**, 150901 (2012).
- [281] A. D. Becke, Perspective: Fifty years of density-functional theory in chemical physics, *J. Chem. Phys.* **140**, 18A301 (2014).
- [282] R. O. Jones, Density functional theory: Its origins, rise to prominence, and future, *Rev. Mod. Phys.* **87**, 897 (2015).
- [283] A. Pribram-Jones, D. A. Gross, and K. Burke, DFT: A theory full of holes? *Annu. Rev. Phys. Chem.* **66**, 283 (2015).
- [284] A. Wasserman, J. Nafziger, K. Jiang, M.-C. Kim, E. Sim, and K. Burke, The importance of being inconsistent, *Annu. Rev. Phys. Chem.* **68**, 555 (2017).
- [285] N. Mardirossian and M. Head-Gordon, Thirty years of density functional theory in computational chemistry: An overview and extensive assessment of 200 density functionals, *Mol. Phys.* **115**, 2315 (2017).
- [286] P. Verma and D. G. Truhlar, Status and challenges of density functional theory, *Trends Chem.* **2**, 302 (2020).
- [287] A. D. Kaplan, M. Levy, and J. P. Perdew, The predictive power of exact constraints and appropriate norms in density functional theory, *Annu. Rev. Phys. Chem.* **74**, 193 (2023).
- [288] P. Bonfà, F. Sartori, and R. De Renzi, Efficient and reliable strategy for identifying muon sites based on the double adiabatic approximation, *J. Phys. Chem. C* **119**, 4278 (2015).
- [289] U. Kuenzer, J.-A. Sorarù, and T. S. Hofer, Pushing the limit for the grid-based treatment of Schrödinger's equation: A sparse Numerov approach for one, two and three dimensional quantum problems, *Phys. Chem. Chem. Phys.* **18**, 31521 (2016).
- [290] A. D. Becke, Density-functional thermochemistry. III. The role of exact exchange, *J. Chem. Phys.* **98**, 5648 (1993).
- [291] F. Jensen, Polarization consistent basis sets: Principles, *J. Chem. Phys.* **115**, 9113 (2001).